NOTE TO USERS

SKELETAL MUSCLES LACKING BPAG1 CROSSLINKING PROTEINS DISPLAY ABERRANT CYTOSKELETAL FEATURES

by
SUZANNE LAMBERT-GIROUX

Thesis submitted in partial fulfillment
of the requirement for the degree of
Master of Science in Human Development (M.Sc.)

School of Graduate Studies
Laurentian University
Sudbury, Ontario

Your file Votre référence
ISBN: 0-494-10030-3
Our file Notre référence
ISBN: 0-494-10030-3

ABSTRACT

Plakin crosslinking proteins have recently emerged as key components of the cytoskeleton. Bullous pemphigoid antigen 1 (Bpag1) is one such protein, identified as the mutated gene responsible for the limb coordination phenotype phenotype observed in *dystonia musculorum (dt)* mice. Given that Bpag1b1/2 molecules, which are the predominant isoforms expressed in contractile tissue, harbor binding sites for the primary components of the cytoskeleton (microfilaments (MF), intermediate filaments (IF), microtubules (MT)), it is argued that Bpag1 proteins interact with MFs, IFs and MTs thereby integrating the functions of these cytoskeletal networks. Accordingly, the impact of Bpag1-deficiency on the expression levels of MF, IF and MT subunits, and the subcellular localization of these cytoskeletal elements was assessed in skeletal muscle.

Analysis of overall mean protein expression levels of actin, desmin and tubulin by Western blotting, reveal that a significant difference in the amount of these proteins detected in skeletal muscle from wild-type, heterozygous and homozygous mice from the dt^{Tg4} transgenic line. In depth analysis of individual protein levels reveal that α-actin and α-tubulin levels are significantly reduced in both slow- and fast-twitch hindlimb muscles of homozygous *dt* mice when compared to wild-type littermates. We also demonstrate that α-tubulin levels are significantly reduced in the soleus slow-twitch muscles of homozygous *dt* mice.

The subcellular localization of MFs, MTs and desmin intermediate filaments was assessed by fluorescence microscopy in order to determine whether the absence of Bpag1

would restructure these cytoskeletal networks in muscle. The absence of Bpag1 resulted in desmin clumping staining patterns and a loss of Z-line staining, uneven α-tubulin staining throughout the cytoplasm as well as attenuated subsarcolemmal staining and uneven actin cytoplasmic staining patterns with a dramatic loss of staining within the subsarcolemmal compartment.

Together, these findings suggest that the absence of Bpag1 negatively impacts the expression levels of muscle cytoskeletal proteins, with specific reductions observed for α-actin and for α-tubulin in skeletal muscle. As hypothesized, all three elements of the cytoskeleton were aberrantly localized as evidenced by abnormal staining patterns in the skeletal muscle of Bpag1-deficient mice. These findings suggest that Bpag1 is involved in regulating the expression levels and cytoskeletal localization of MFs, desmin IFs and MTs in skeletal muscle. These architectural modifications are likely responsible for the development of the post-natal myopathy that occurs in homozygous *dt* mice.

ACKNOWLEDGEMENTS

Special thanks to my supervisor, Dr. Céline Boudreau-Larivière, an amazing professor, friend and mentor. You dedicated countless hours to my work and inspired me daily to pursue my research. I will be forever grateful for the way you have impacted my life and your patience throughout this experience is truly appreciated. You are a true mentor and inspiration and I feel so fortunate to have worked under your guidance. Milles merci 'teacher'!

Thanks to members of my advisory committee, Drs Olivier Serresse and Run-Min Zhou, for their helpful comments and their time in reviewing my progress. In addition, I thank Dr. Zhou for his guidance with the statistical analyses. I also wish to extend my gratitude to Chris Blomme and Nicole Paquette for their help with the animals and all their wonderful support and involvement with the animal care facility.

To my parents who've been there for me since the very beginning. I have been blessed with a mother and father that have supported and encouraged me in all aspects of life. Thanks for all the pep talks, wiping away the tears and just being there.

Last but certainly not least, to my husband Curtis, thank you for your continuous support, faith, love and friendship. You kept me strong when I was tired and were always there when I needed you. I love you and thank you.

TABLE OF CONTENTS

LIST OF FIGURES

LIST OF TABLES

LIST OF ABBREVIATIONS

ABD – Actin-binding domain
ACTA1 – Skeletal muscle alpha-actin gene
Bpag1 – Bullous pemphigoid antigen 1
Bpag1-a & -n – Neural isoforms
Bpag1-b – Muscle isoform
Bpag1-e – Epithelial isoform
BR – Bradford reagent
BSA – Bovine Serum Albumine
CC rod domain – Coiled coil rod domain
DNA – Deoxyribonucleic acid
dt – *Dystonia musculorum*
dt^{24J} – 24 Jackson
dt^{27J} – 27 Jackson
dt^{Alb} – Albany
dt^{Frk} - Frankel
DRG – Dorsal root ganglia
F-actin – Filamentous-actin
G-actin – Globular-actin
IF – Intermediate filament
IFBD – Intermediate-filament binding domain
kb – kilo-base
kD – kilo-Dalton
MACF – Microtubule-actin crosslinking factor
MF – Microfilament
mRNA – Messenger ribonucleic acid
MT – Microtubule
MTBD – Microtubule-binding domain
MTJ – Myotendinous junction
MURF – Muscle-specific RING-finger protein
MyHC – Myosin heavy chain
NF – Neurofilament
PD – Plakin domain
PCR – Polymerase chain reaction
PVDF – Polyvinylidene fluoride microporous membrane
PRD – Plectin repeat domain
SR – Spectrin repeat
T-tubules – Transverse tubules

Introduction

The cytoskeleton refers to the architectural framework of cells. It is this framework that is largely responsible for the diversity in the shape, size, and function of cells in multicellular organisms. Microfilaments (MF), intermediate filaments (IF), and microtubules (MT), are the primary cellular components of the cytoskeleton and collectively, these elements play important roles in cellular division, cell motility and in the establishment and maintenance of cellular structural integrity. Until recently, these main cytoskeletal networks had been viewed as distinct elements each functioning independently from one another. A more contemporary view of the cytoskeleton is one that highlights the interconnectedness of these primary filamentous networks whereby disruption of one cytoskeletal element impacts the others. In this context, linker molecules that interconnect the primary cytoskeletal components have been identified and their role in crosslinking MFs, IFs and MTs, and thereby integrating their functions, has only recently begun to be described. The present study is aimed at elucidating the role of one such crosslinking protein; namely Bullous pemphigoid antigen 1 (Bpag1).

Cytoskeletal Elements in Skeletal Muscle Tissue

1) Basic Cellular Components of Skeletal Muscle

Skeletal muscle fibers are made up of elongated muscle cells, with nuclei lying directly below the sarcolemma (the muscle fiber's plasma membrane). The muscle

fiber's cytoplasm is filled with mitochondria and myofibrils. It is the latter which contains the filamentous network that enables spatial organization and which comprises the framework of the cell. Each myofibril is surrounded by a sarcoplasmic reticulum, a saclike membranous network, and is closely associated with transverse tubules (T-tubules) which penetrate the cell's interior via their connection with the sarcolemma. Both sarcoplasmic reticulum and T-tubules are important structures in the excitation-contraction coupling process.

Myofibrils are composed of a fundamental unit called a sarcomere (Clark et al. 2002). The sarcomere, which consists of contractile, cytoskeletal, and associated regulatory proteins, is the basic contractile unit of the mature skeletal muscle fiber (Figure 1). The principle components of the sarcomere include parallel arrays of actin-containing thin filaments spanning the I-band, and myosin-containing thick filaments in the A-band. The I-band region is responsible for linking the A-band, the region of active force generation, with the Z-lines. Each sarcomere is bordered on either end by Z-lines, running perpendicular to the long axis of myofibrils, which anchor the thin filaments. Thus, Z-lines are arranged adjacently in myofibrils, enabling the coordination of muscle contractions between individual myofibrils to where the Z-line is linked to the muscle membrane. The IF-rich Z-line is an important area for signaling and muscle homeostasis. M-lines, which also run perpendicular to the long axis of myofibrils, are responsible for connecting thick filaments together and their appearance is considered to define the final step in myofibril assembly (Markwald 1973).

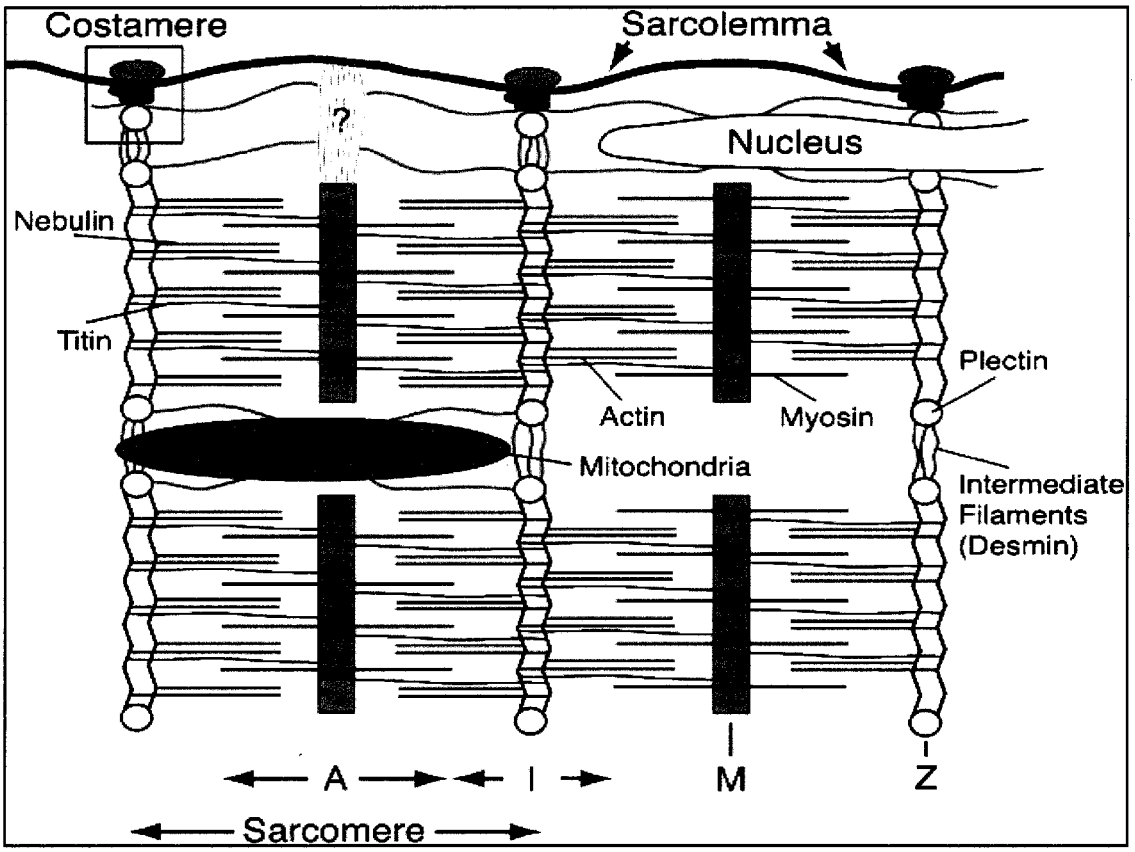

Figure 1 Schematic representation of the cytoarchitectural design of the skeletal muscle fiber (from Clark et al., Annu. Rev. Cell Dev. Biol., 2002).

Costameres, another feature of striated muscle, are distinct subsarcolemmal units that appear to connect the sarcolemma to the extracellular matrix thereby anchoring predominantly Z-lines (Berthier and Blaineau 1997) and providing organizational points for the membrane cytoskeleton (Figure 1). Skeletal muscle myofibrils terminate at the myotendinous junction (MTJ), another area linked to the plasma membrane. The MTJ is the focal point of force transmission during muscle contraction. Although specific functions are attributed to the various cellular components found in skeletal muscle, collectively these elements function in unison and are therefore interdependent to ensure optimal muscle contraction while maintaining the overall structural integrity of this tissue during these episodes of significant mechanical stress.

2) Cytoskeletal Elements in Fast- versus Slow-Twitch Muscle Fibers

Skeletal muscle fibers are composed of numerous types of muscle fibers that dictate the overall contractile properties of muscles (Pette and Staron 2001). These fiber types can be distinguished from one another based on various parameters including molecular, metabolic, structural, and contractile. The muscle fibers are most often classified as Type I and Type II, with the latter having at least three major types (IIA, IIB, and IIX – also known as IID), according to the specific myosin heavy chain (MyHC) isoforms expressed, which reflects the level of activity of myofibrillar adenosine triphosphatase. Type I fibers, referred to as slow-twitch fibers, are capable of generating limited force and contract relatively slowly for prolonged periods of time. Postural muscles, such as the soleus leg muscle, contain primarily Type I fibers. Conversely,

Type II fibers, collectively regarded as fast-twitch fibers, have the ability to generate more force and contract much more quickly for limited periods of time. Muscles involved in explosive movements such as the gastrocnemius are composed primarily of Type II fibers. It is worth noting that muscle fibers can undergo significant changes in their phenotype when subjected to modifications in neuromuscular activity, mechanical loading and exposure to specific hormones, as well as aging (Pette and Staron 2001).

Differences between Type I and Type II fibers are not limited to metabolic and contractile properties. Fiber type-dependent differences in other elements of the muscle fiber, notably the cytoskeleton, have also been highlighted. For example, immunoblotting experiments by Boudriau et al. (1993) have demonstrated higher concentrations of α-tubulin, a subunit protein of MTs, in Type I muscle fibers when compared to Type II fibers. While no significant differences were observed in the spatial orientation and organization of MTs between Type I and Type II fibers as revealed by immunofluorescence analysis of muscle sections, it was noted that the density of MTs within the sarcoplasmic and subsarcolemmal space was greater in Type I versus Type II fibers. Denser bundles of MTs around the myonuclei and within the subsarcolemmal region of Type I fibers of rat soleus muscle compared to Type II fibers of the rat tensor fascia latae muscles was also recently reported (Ralston et al. 1999). Other examples of fiber type-dependent differences related to cytoskeletal proteins include the higher abundance reported for desmin IF and for dystrophin, a membrane-linked cytoskeletal protein, in Type I versus Type II fibers (Ho-Kim and Rogers 1992; Chopard et al. 2001). The higher content of various cytoskeletal proteins in slow-twitch fibers possibly

underscores the need for enhanced structural stability in muscles that undergo lengthier periods of mechanical stress. Thus, it remains likely that genetic mutations causing cytoskeletal disturbances may have a greater impact on Type I muscle fibers.

Primary Components of the Cytoskeleton

1) Actin Microfilaments

Actin microfilaments, measuring 6 nm in diameter, are comprised of two strands of polymerized globular actin monomers which form a double helix (Figure 2). Actin microfilaments are involved in various cellular functions including cell motility, muscle contraction, and separation of the cytoplasm during cell division. Two factors underlying actin microfilament dynamics include: 1) the ability to undergo reversible transformations from the monomeric state (Globular-actin or G-actin) to the polymeric state (Filamentous-actin or F-actin), and 2) the ability to interact with actin-binding proteins (Sheterline et al. 1995). Multiple actin isoforms namely α–actin, β–actin, and γ–actin are synthesized in various cell types and can be classified as sarcomeric (found within the sarcomere) or exosarcomeric/cytoplasmic (found outside the sarcomere). The isoforms are highly similar in their amino acid sequences and molecular structures. Despite the segment similarities, these actin isoforms are functionally different (Khaitlina 2001). The various actin isoforms are expressed in a tissue-specific manner. Gamma (γ) actin is found predominantly in smooth muscle and nonmuscle cells (Storti et al. 1976; Rubenstein and Spudich 1977), β-actin is more highly expressed in

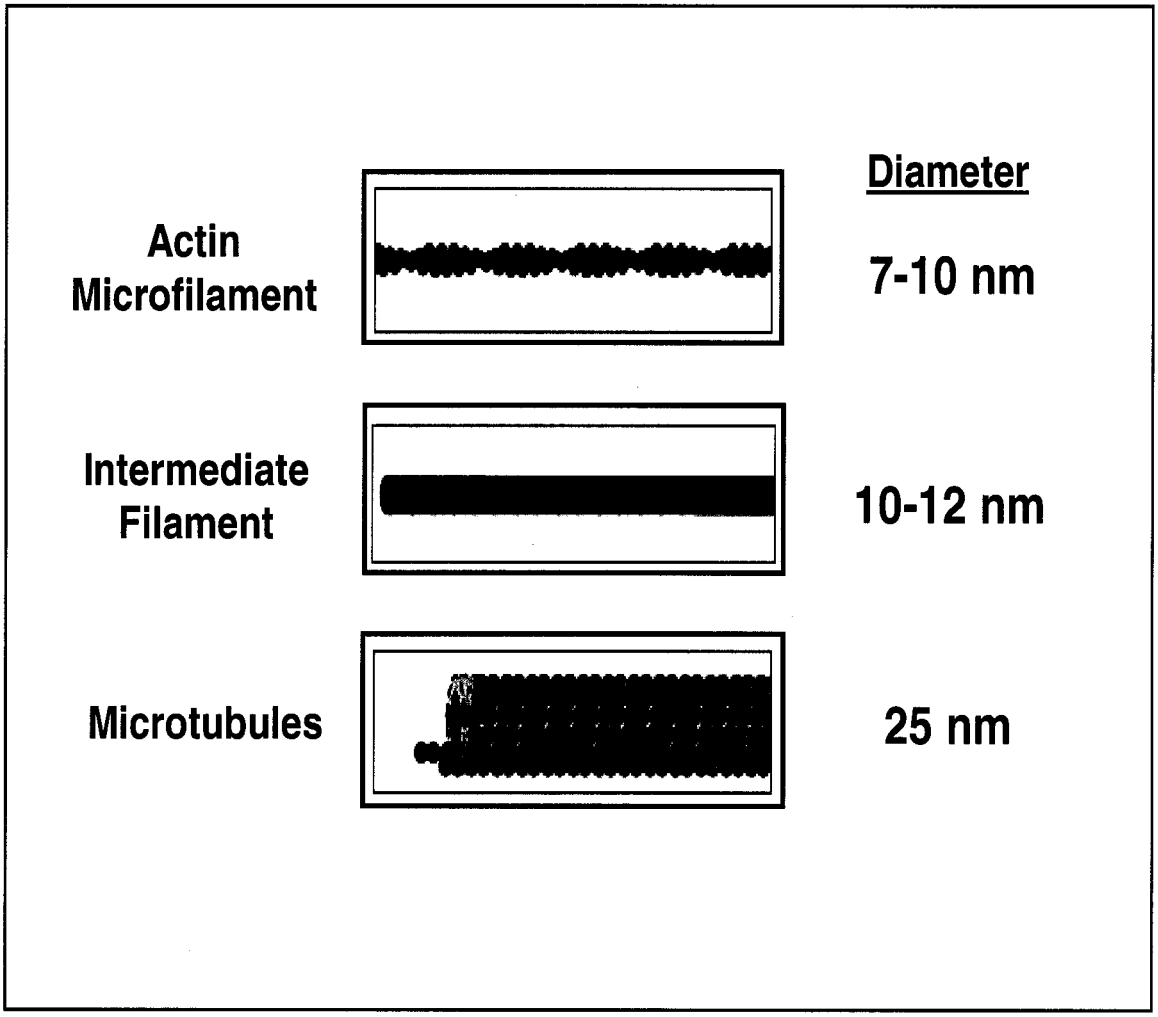

Figure 2 Schematic representation of the primary components of the cytoskeleton. (A) Actin MF consists of two helically arranged strands of F-actin. (B) IFs are composed of small elongated rod-like dimmers. (C) MTs are globular tubulin heterodimers that form a long hollow tubule. (Modified from German and Stanfield, Principals of Human Physiology, 2002)

nonmuscle cells (Storti et al. 1976; Rubenstein and Spudich 1977), and α-actin is mostly expressed in skeletal and cardiac muscle and is therefore the distinct sarcomeric isoform (Vandekerckhove and Weber 1979).

Mutations in striated muscle actin isoforms can result in various forms of human myopathies depending on the domain affected. For example, different mutations in the skeletal muscle α-actin gene (ACTA1) are associated with actin myopathy and nemaline myopathy in humans (Nowak et al. 1999; Ilkovski et al. 2001). Although characterized by myofibrillar structural abnormalities and muscle weakness, clinical phenotypic variability among patients suggests that both the site of the mutation and the nature of the amino acid change have differential effects on thin-filament formation and protein-protein interactions (Ilkovski et al. 2001). It is clear that actin plays an important role in maintaining cellular structure and integrity however, the interaction of actin with other cytoskeletal proteins and the impact of this association on MF function remains to be fully described.

2) Intermediate Filaments

Intermediate filaments have a diameter of approximately 10 nm and are named as such because their size is intermediate between that of MFs and MTs. These filaments are made up of small elongated rod-like dimers which provide cells mechanical strength and resistance to stress (Fuchs and Weber 1994). There are various classes of intermediate filaments that differ from one another based on their subunit composition.

Furthermore, these various types of IFs are differentially expressed in tissues and cell types. IFs are classified into 5 major types according to their sequence similarities. Types I to IV are cytoplasmic IFs, while Type V are nuclear IFs. For example, keratin filaments, which are classified as type I (acidic) or type II (basic) IF proteins, are synthesized in epithelial cells and represent the major differentiation product of the epidermis (Lazarides 1980a). Neurofilaments as well as glial filaments are classified as type IV IF proteins and are expressed in neurons and all types of glial cells respectively. Type V IF proteins are lamins which form the nuclear lamina and seemingly provide a framework for the cell's nucleus (Fuchs and Weber 1994).

Other intermediate filaments classified as type III IF proteins are vimentin (Franke et al. 1978; Yang et al. 1996), nestin (Sejersen and Lendahl 1993; Zimmerman et al. 1994), paranemin (Price and Lazarides 1983) and synemin (Bilak et al. 1998), all of which are expressed in striated muscle, as well as peripherin, which is expressed in neural cells (Portier et al. 1983). Peripherin is found in the peripheral nervous system and is localized with ventral motor neurons, neurons of the dorsal root ganglia, sympathetic neurons, and cranial nerves (Portier et al. 1983). Vimentin, which is transiently expressed during muscle development, is believed to be tightly associated with the cell nucleus (Granger and Lazarides 1979; Lazarides 1980b). Nestin, paranemin, and synemin are also expressed during muscle development, with nestin and vimentin being up regulated during fiber regeneration (Sjoberg et al. 1994). Although type III intermediate filaments play important roles with regard to proper cytoskeletal functioning

and maintenance in striated muscle, desmin is likely the most well studied and characterized of the type III IFs.

Desmin is a component of the Z-line, costameres, and the myotendinous junction of skeletal muscle, as well as a component of intercalated discs of cardiac muscle (Lazarides 1980a). In mature striated muscle, desmin is known to link myofibrils adjacently as well as with the sarcolemma (Granger and Lazarides 1978). Ultrastructural studies also demonstrate its ability to form connections with mitochondria, nuclei and other organelles (Tokuyasu et al. 1983). Research on desmin-null mice have revealed post-natal musculoskeletal abnormalities in the form of lateral myofibril mis-alignment, increased myofibrillar mobility, disrupted myofibril-sarcolemma anchorage, intercalated disc deviations, deformed and irregularly positioned mitochondria, as well as cardiac muscle degeneration and necrosis (Li et al. 1997; Milner et al. 1999; Balogh et al. 2002; Shah et al. 2002). Based on these and related studies, it is clear that desmin intermediate filaments play a key role in maintaining the functional and architectural integrity of striated muscle by ensuring myofibrillar integrity and structural alignment.

Other more recently identified IF proteins expressed in muscle include desmuslin, syncoilin (Mizuno et al. 2001; Newey et al. 2001; Poon et al. 2002), and cytokeratins (Kosmehl et al. 1990). The need for such a wide variety of IFs is not entirely clear, but may underscore tissue- as well as developmentally-specific requirements. It may also indicate the need for compensatory or back-up IF molecules in the event that one IF is aberrantly expressed.

3) Microtubules

Microtubules, the largest filaments measuring 23 nm, are polymers made-up of α– and β–tubulin heterodimers (Stephens and Edds 1976). Although known for providing strength to the cytoskeleton, they also play a role in cell motility, organelle positioning, intracellular transport, and chromosome distribution during mitosis. In skeletal muscle, MTs are positioned between myofibrils and are also associated with nuclei, the Golgi complex and the sub-sarcolemmal region (Clark et al. 2002). Furthermore, disruption of microtubule dynamics compromises myoblast fusion and differentiation (Antin et al. 1981; Saitoh et al. 1988). More recent studies are suggesting the possible role of muscle microtubule-associated proteins, such as M-cadherin and muscle-specific RING-finger protein (MURF), as key components in stabilizing and organizing MTs (Kaufmann et al. 1999; Spencer et al. 2000). The stability and cellular localization of MTs in skeletal muscle is also likely to be dependant on other cytoskeletal components that possess MT-binding activity.

Plakins

The concept of cytolinker or crosslinking proteins has been advanced in the past (Ellisman and Porter 1980; Hirokawa 1982), but only recently has distinct evidence for their existence been demonstrated. Besides MFs, IFs and MTs, proteins belonging to the plakin family have recently emerged as key components of the cytoskeleton. Plakin crosslinking proteins are expressed in a variety of tissues, notably those that undergo

significant mechanical stress such as muscle and skin, though not limited to these tissue types. Thus, diseases where synthesis of the linker proteins is perturbed are often characterized by various forms of tissue fragility for example, skin blistering (Minoshima et al. 1991). Presently, there are seven known plakin family members including: desmoplakin, plectin, envoplakin, periplakin, epiplakin, bullous pemphigoid antigen 1 (Bpag1) and microtubule-actin crosslinking factor (MACF, also known as Acf7) (Ruhrberg and Watt 1997; Leung et al. 2001a; Leung et al. 2002). Several of these sequence-related molecules exist as families of tissue-specific isoforms generated through alternative splicing of their respective genes (Figure 3).

Plakin family members share two common regions. One area is defined as the plakin domain and the other region is referred to as the plectin repeat domain (PRD) (Leung et al. 2001a). The plakin domain, which is situated mostly at the N-terminus of molecules, possesses sites that either directly or indirectly mediate binding to adhesion molecules such as integrins (Rezniczek et al. 1998; Geerts et al. 1999). In certain plakin family members such as periplakin and plectin, the PRD is found at the C-terminus of these proteins, whereas in larger plakin proteins such as MACF and most Bpag1 isoforms, this domain is centrally located (Schultz et al. 1998; Leung et al. 2001a). The only known function to date of the PRD is that of binding intermediate filaments (Ruhrberg and Watt 1997; Leung et al. 2002), but additional functions are suspected (Roper et al. 2002).

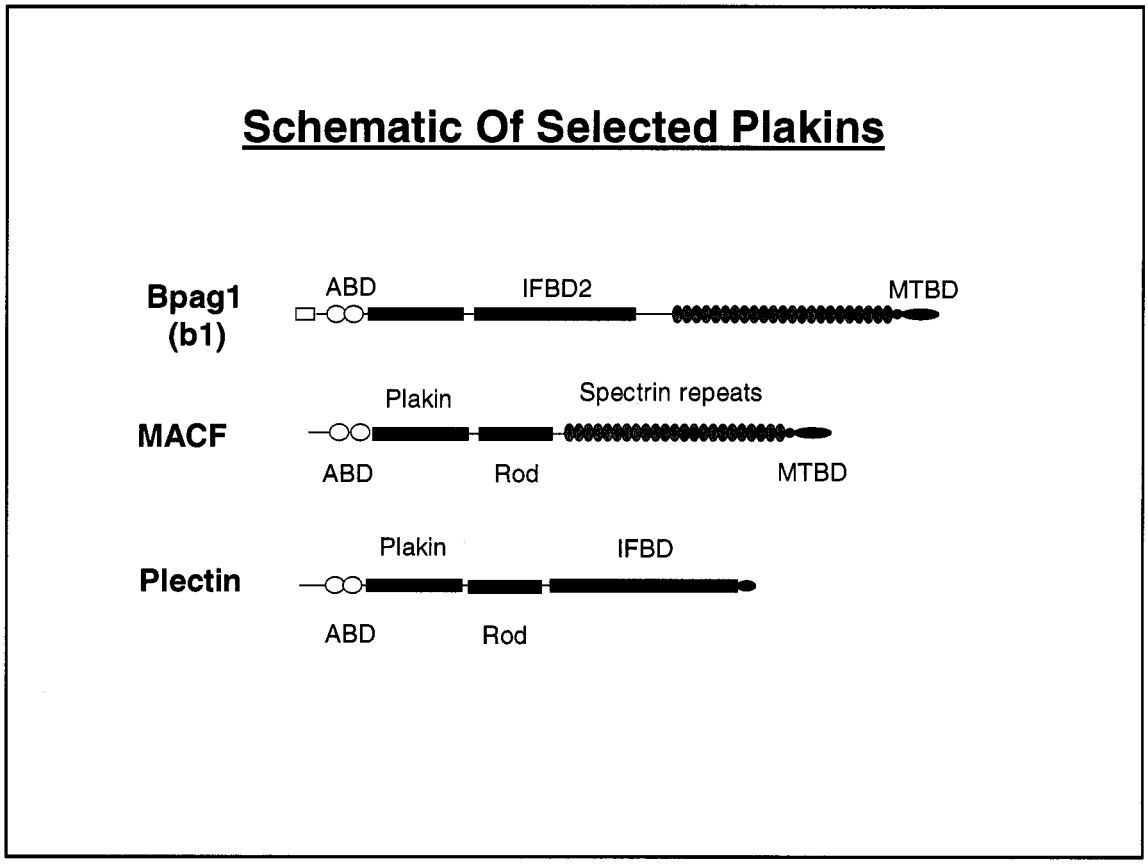

Figure 3 Schematic representation of selected plakin family members including Bpag1, MACF and plectin. Note the common interaction domains. Abbreviations are ABD; the actin-binding domain, IFBD1 and 2; the intermediate filament-binding domain and MTBD; the microtubule-binding domain.

1) Spectraplakins

A recent review has grouped Bpag1 and MACF into a subfamily of proteins called 'spectraplakins' (Roper et al. 2002). This subcategory distinguishes Bpag1 and MACF from other plakins based on the fact that these molecules possess spectrin repeats. The spectrin-repeat domain is a three-helix bundle that forms a so-called spacer rod. The function of this domain is to separate the various functional domains of the molecule (Pascual et al. 1997). Another feature of spectraplakins is the presence of an N-terminal actin-binding domain (ABD). In this context, it is worth mentioning that plectin also harbors an ABD at the N-terminus and therefore is suspected to be a third spectraplakin, although the presence of spectrin repeats in plectin molecules has yet to be demonstrated. Because of the large size of these proteins, and given that they harbor binding sites for the primary components of the cytoskeleton (MFs, IFs and MTs), it is argued that spectraplakins, in particular Bpag1 proteins, interact with microfilaments, intermediate filaments and microtubules thereby integrating the functions of these cytoskeletal networks (Leung et al. 2002).

Bullous Pemphigoid Antigen 1 (Bpag1)

The term Bpag1 refers to the antigen targeted by auto-antibodies in a human skin blistering illness known as *Bullous Pemphigoid.* Bpag1, also known as dystonin, was identified by two independent groups as the mutated gene responsible for the *dystonia musculorum (dt)* phenotype observed in mice, as discussed on page thirty (Brown et al.

1995; Guo et al. 1995). The Bpag1 gene in mice spans approximately 500 kb (kilo-base) and is situated on chromosome 1 (Brown et al. 1995; Leung et al. 2001b). The Bpag1 gene encodes several different interaction domains including a plakin domain, an actin binding domain (ABD), a coiled coil (CC) rod domain, a microtubule-binding domain (MTBD), a spectrin repeat (SR)-containing rod domain, and two potential intermediate filament-binding domains (IFBD1 & IFBD2) (Leung et al. 2001b). Some regions, notably the plakin domain, are encoded by multiple exons while other domains, such as IFBD2, are encoded by single large exons (Leung et al. 2001b). Interestingly, the gene encodes multiple isoforms that are generated by alternative splicing.

1) Bpag1 Isoforms

The Bpag1 gene encodes multiple isoforms including an epithelial isoform (Bpag1e), neural isoforms (Bpag1a, Bpag1n), and muscle isorforms (Bpag1b) (Figure 4). While these isoforms share common features, they also possess distinct structural elements that are thought to fulfill specific functions. This may be due in part to the unique function of the N-terminal domain in dictating the function and localization of Bpag1 isoforms (Young et al. 2003).

The epithelial isoform, termed Bpag1e, is expressed in epithelial cells of the skin (Yang et al. 1996; Dalpe et al. 1998; Leung et al. 2001b). The smallest of the isoforms with a molecular mass of 302 kD (kilo-Dalton) and a transcript size of 8.6 kb, Bpag1e contains a plakin domain, common to all plakins, with the addition of a COOH-terminal

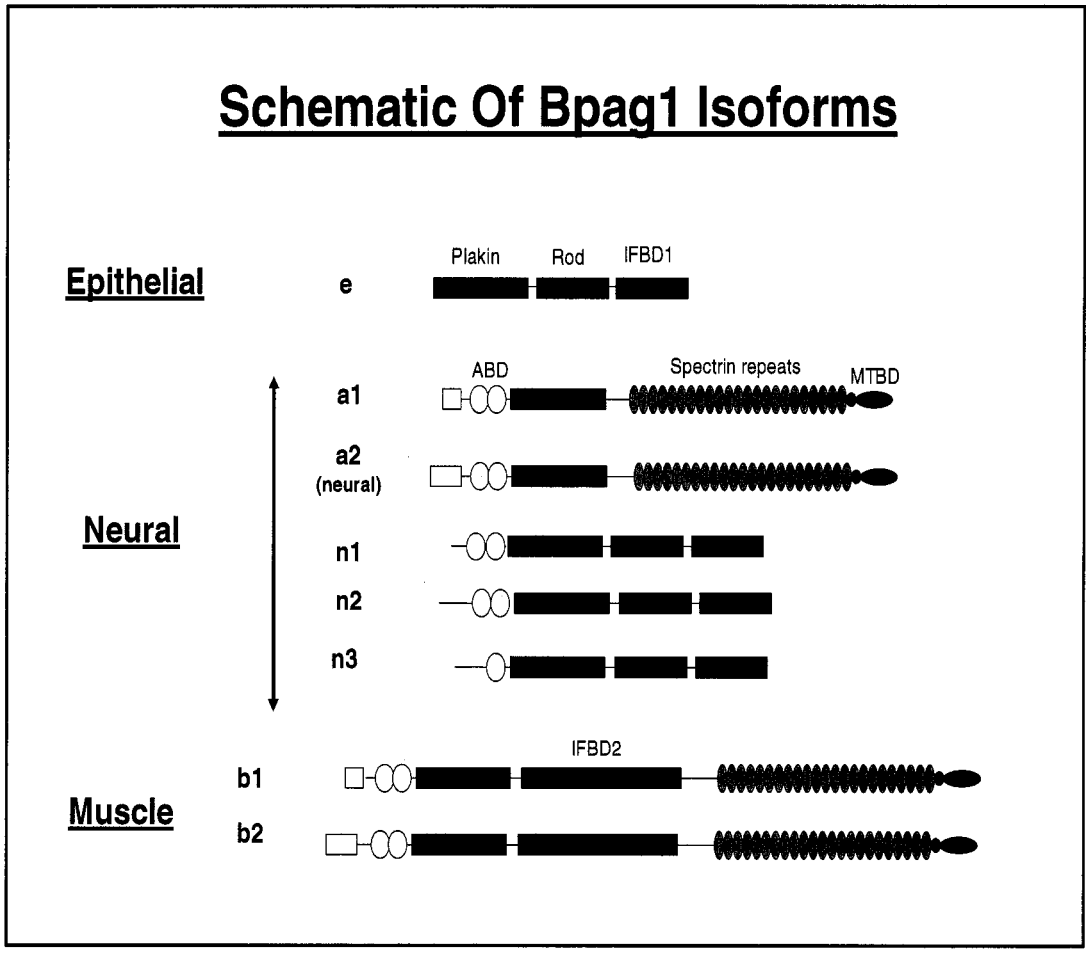

Figure 4 Schematic representation of Bpag1 isoforms. Abbreviations are ABD; the actin-binding domain, IFBD1 and 2; the intermediate filament-binding domain and MTBD; the microtubule-binding domain. (Modified from Leung et al., J. Cell Biol., 2001b)

tail domain consisting of two homologous spectrin repeats, proposed to be an intermediate filament binding domain (IFBD) (Leung et al. 2001b) (Figure 4). In this context, Bpag1e has been shown to be involved in the anchoring of keratin intermediate filaments to hemidesmosomes (Mueller et al. 1989; Jones et al. 1994). Further evidence supporting this keratin-IF binding function, is the observation that Bpag1-null mice display increased skin blistering (Guo et al. 1995).

The neuronal isoforms, bpag1a1 and bpag1a2, are encoded by transcripts of approximately 17.2 kb in length (Figure 4). The protein products in turn are estimated to be 615 kD (Leung et al. 2001b). These isoforms differ in their N-terminal regions (Brown et al. 1995) but share a common ABD, made up of 2 calponin homology domains, a spectrin-repeat domain (Leung et al. 2001b) and a microtubule-binding domain (MTBD) at the C-terminus (Yang et al. 1996; Leung et al. 1999; Leung et al. 2001b). Bpag1a isoforms are mainly expressed in the nervous system and the dorsal root ganglia (DRG), and their absence is likely the primary cause of the neurological phenotype reported in *dt* mice (Leung et al. 2001b).

Bpag1n isoforms (Bpag1n1, n2, n3 and n4) are additional neuronal isoforms that are encoded by mRNAs approximately 9.6 kb in size which produce proteins with a molecular mass of 344 kD (Leung et al. 2001b; Young et al. 2003; Jefferson et al. 2004). The Bpag1n1 and –n2 isoforms are made up of an N-terminal ABD, a plakin domain, a CC-rod domain, and an IFBD at the C-terminus (Leung et al. 2001b). Bpag1n1 and –n2 are reportedly minor isoforms expressed in neural tissue (Brown et al. 1995; Leung et al.

2001b). Bpag1n3 is structurally similar to bpag1n1 and –n2 however, it contains a unique 5' region followed by a single calponin homology subdomain of the ABD which abolishes the actin binding activity of this region (Yang et al. 1999).

Muscle isoforms Bpag1b1 and –b2, are encoded by 22.2 kb transcripts which produce large proteins of approximately 824 kD (Leung et al. 2001b). They are structurally similar to Bpag1a isoforms, with the addition of a novel IFBD (IFBD2) located at the center of the molecule (Leung et al. 2001b). Although detected in other cell types, including the nervous system, Bpag1b is the predominant isoform expressed in striated muscle (Dalpe et al. 1998; Dalpe et al. 1999; Leung et al. 2001b). Given that Bpag1b isoforms harbor an ABD, an IFBD and a MTBD, it is highly likely that this gigantic crosslinking molecule is able to associate with actin-MFs, desmin-IFs, and MTs thereby integrating the functions of the primary cytoskeletal components. However, evidence for this notion remains to be clearly established.

2) Specialized Domains of Bpag1 Isoforms Bind to Cytoskeletal Elements

The functions of some of the protein domains of Bpag1 isoforms have been revealed using a variety of experimental approaches. Biochemical and molecular analyses have in fact demonstrated that the ABD and the IFBD1 are functional in that they can bind to actin MFs and IFs respectively. Actin binding assays, for example, using polymerized actin and fusion proteins containing the ABD of Bpag1, have revealed a high level as well as a specific degree of association between MFs and the ABD (Yang

et al. 1996). Mini fusion proteins containing the ABD and IFBD1 have been shown to co-align MFs and desmin IFs in cultured COS-1 cells derived from monkey kidney cells (Dalpe et al. 1999). Furthermore, a full length version of Bpag1-n, harboring both the ABD and the IFBD1, has been reported to restructure the neurofilament and actin networks in adrenal carcinoma cells, resulting in the co-localization of Bpag1n, actin MFs and NFs as revealed by immunofluorescence staining (Yang et al. 1996). Intermediate filament (IF) binding activity has yet to be ascertained for IFBD2 although its structural similarity to IFBD1 would predict the ability of IFBD2 to effectively interact with IFs.

Using transfected COS-7 cells, the MTBD has been shown *in vitro* to stabilize the MT network by binding to microtubules (Sun et al. 2001). A tagged fusion protein expressing the MTBD of Bpag1 co-localizes with endogenous MTs in transfected COS-7 cells as revealed by immunofluorescence experiments (Sun et al. 2001). Furthermore, in the presence of MTBD fusion proteins, MTs appear to be protected from a MT destabilizing agent known as nocodazole, thereby suggesting that the MTBD can interact with and stabilize MTs. Collectively, these studies provide evidence for specific binding abilities of individual protein domains (i.e. ABD, IFBD1, MTBD). However, evidence to confirm a definitive role of Bpag1 in binding all three cytoskeletal components simultaneously has yet to be reported.

3) *Dystonia Musculorum (dt)* Mouse

Dystonia musculorum (*dt*), first described by Duchen (1964) as an autosomal recessive condition, has been classically viewed a sensory neuropathy of the mouse. Born with normal physical appearance, these mice first display signs of physical abnormalities at approximately post-natal day 7 to 10. Mice that are homozygous for the *dt* allele show progressive loss of limb coordination and when lifted by their tails, flex their hindlimbs toward the trunk of the body (Figure 5). In addition to this phenotype, these mice display twisted forelimbs with the foot held in a hyper-pronated position, as well as jerky and uncoordinated movements (Duchen et al. 1964; Duchen 1976). By three weeks of age, these mice die of unknown causes (Duchen et al. 1964; Duchen 1976).

There are currently six known *dt* alleles, four of which are spontaneous mutations that have appeared in different mouse strains. For instance, 24 Jackson (dt^{24J}) (Brown et al. 1995) and 27 Jackson (dt^{27J}) (Duchen 1976) emerged from a C57BL/6 strain, Albany (dt^{Alb}) (Messer and Strominger 1980; Brown et al. 1995) from a Balb/c mouse strain, and Frankel (dt^{Frk}) arose by spontaneous mutation on a DBA background. The genetic alterations have not yet been described for these spontaneous mutants. A fifth *dt* allele is the Bpag1 knock-out (-/-) mouse model, generated by homologous recombination, targeting the N-terminus of the epithelial isoform of Bpag1 (Guo et al. 1995) which abolishes gene expression at the Bpag1 locus. A sixth allele is the dt^{Tg4} mouse model, which was generated inadvertantly when a transgene insertion caused a mutation at the *dt*

Figure 5 Dystonia musculorum (dt^{Tg4}) mouse model. Compared to the wild-type littermate (right), the homozygous mouse (left) is smaller and displays an arching of the spine and hyperflexion of the limbs as reflected by twisting movements of the trunk.

locus of a CD-1 mouse strain (Kothary et al. 1988). Characterization of the integration site of the transgene led to the identification of Bpag1 as the defective gene (Brown et al. 1995). It should be noted that mutations of genes encoding plakin crosslinking proteins are associated with several diseases including skin blistering disorders and muscular dystrophy in humans and neuronal degeneration in mouse mutant models. Interestingly, independent mutations within distinct regions of the Bpag1 locus result in similar phenotypic outcomes in *dt* mice (i.e. limb incoordination, death by 3-4 weeks post-natal).

Mutations at the Bpag1 locus have an impact on gene expression that is manifested as a dramatic reduction in the level of Bpag1 mRNA in brain, spinal cord, sciatic nerve, epithelium and skeletal muscle (Guo et al. 1995; Yang et al. 1996; Bernier and Kothary 1998; Dalpe et al. 1998; Dalpe et al. 1999). Although the precise molecular mechanisms leading to this loss of Bpag1 mRNA has not yet been fully characterized, abolishment of Bpag1 gene transcription is the most probable event.

4) Proposed Functions of Bpag1 Isoforms

Studies using the *dt* mouse model have begun to describe the important function of Bpag1 gene products in a variety of cell types including epithelial, neural, and muscle cells. To date, most studies using the *dt* mouse model have described the epithelial and neuronal phenotypes which will be reviewed in the following two sections. The muscle phenotype is less well characterized and is of particular relevance to the proposed study aimed at further defining the role of Bpag1 in skeletal muscle.

(a) Epithelial tissues

The epithelial isoform of Bpag1 is predominantly localized to the intracellular portion of the hemidesmosomal plaque, a region which associates keratin filaments (Stanley 1993). Ultrastructural analysis of basal skin cells in mice lacking Bpag1 reveal mild blistering of the tail, as well as the absence of keratin filaments at hemidesmosomal plaques, however cells lacking Bpag1e have hemidesmosomes with seemingly normal structure (Guo et al. 1995). Thus, Bpag1 provides mechanical strength at the base of an epidermal cell by acting as an anchor for the IF network. Although the removal of Bpag1 does not perturb cell-substratum adhesion, it does however have an affect on other proteins which become ineffective at connecting the IF network to the plaque (Guo et al. 1995).

(b) Neural tissues

Results of histopathological studies reveal that dorsal roots and dorsal root ganglia of *dt* homozygous mice are smaller compared to wild type littermates (Duchen et al. 1964; Duchen 1976). In addition, *dt* mice show signs of neurodegeneration as evidenced by axonal swellings and fibrosis in the dorsal roots (Janota 1972; Duchen 1976). Hallmarks of the disease include accumulation of neurofilaments, organelles and empty vacuoles in axonal swellings (Janota 1972; Kothary et al. 1988; Sotelo and Guenet 1988; Campbell and Peterson 1992). Secondary sensory neurons in the spinal cord are also affected showing signs of axonal swellings, chromatolytic changes, and neuronal

atrophy (Sotelo and Guenet 1988; al-Ali and al-Zuhair 1989). Schwann cells are also affected in *dt* mice as evidenced by hypo/amyelinated peripheral nerves, abnormal polarization and matrix attachment, and a disorganized Schwann cell cytoskeleton (Bernier et al. 1998).

Studies reveal disorganization of the neurofilament and microtubule networks within the dorsal roots of *dt* mice as early as embryonic day 14 (Bernier and Kothary 1998; Dalpe et al. 1998), thereby indicating that cytoskeletal disorganization precedes neurodegeneration (Dalpe et al. 1998; Dalpe et al. 1999). Furthermore, both in vivo and in vitro studies demonstrate that abolishing neurofilament expression does not attenuate the disruption of the microtubule network in sensory axons of Bpag1 -/- knock-out mice (Yang et al. 1999). This observation suggests that defects in the microtubule network are primarily attributable to the absence of Bpag1 expression rather than a secondary outcome of neurofilament disorganization (Yang et al. 1999).

It is generally thought that motor neurons remain largely unaffected by Bpag1-deficiency (Dowling et al. 1997). When signs of motor neuron degeneration have been reported, it has been postulated that it is a secondary outcome of sensory neurodegeneration. Furthermore, it is likely that motor neurons are protected from degeneration due to the compensatory effect of other plakins, such as MACF, that are expressed in these neural cells. Experiments designed to abolish expression of Bpag1 and MACF simultaneously in motor neurons will be helpful in addressing this issue.

It has been hypothesized that disruption of the neurofilament and MT networks in sensory neurons would have a functional impact on axonal transport (Bernier and Kothary 1998; Dalpe et al. 1998). This hypothesis was in fact recently confirmed. Orthograde and retrograde transport of acetylcholinesterase in the sciatic nerves of *dt* mice, compared to the sciatic nerves of wild-type mice, was found to be hindered (De Repentigny et al. 2003).

(c) Skeletal muscle tissues

Bpag1-deficient mice are born with overall intact skeletal muscle tissue (Dalpe et al. 1999). However, pronounced sarcomeric disorganization observed by ultrastructural analysis both in vitro and in vivo, indicate a likely role of Bpag1 in maintaining the structural integrity of skeletal muscle cells (Dalpe et al. 1999). It should be noted that myogenic cell differentiation and growth are unaffected in the absence of Bpag1 (Boudreau-Lariviere and Kothary 2002). Taken together, these observations suggest that Bpag1 plays a role in the maintenance rather than the establishment of the muscle cell architecture (Dowling et al. 1997; Dalpe et al. 1999; Boudreau-Lariviere and Kothary 2002).

It should be noted that the skeletal muscle phenotype of *dt* mice occurs independently of the neuropathy. Specifically, motoneurone degeneration is nearly absent in *dt* mice (Bernier et al. 1995; Dowling et al. 1997) thereby indicating that ultrastructural disorganization of skeletal muscle is not the result of muscle denervation

(Dalpe et al. 1999). Expression levels of denervation markers, such as myogenin and acetylcholinesterase, are not affected in *dt* skeletal muscle tissue. More specifically, in skeletal muscle of *dt* mice, myogenin mRNA levels are not up-regulated and acetylcholinesterase activity remains comparable to that observed in wild-type skeletal muscle tissue (Dalpe et al. 1999; De Repentigny et al. 2003).

5) Impact of Bpag1-Deficiency on the Sarcolemmal Integrity and Contractile/Metabolic Properties of Skeletal Muscle

In vitro assessment of contractile properties of the diaphragm muscle of *dt* mice reveal pronounced sarcolemmal damage following a fatigue protocol, when compared to their wild-type litter mates (Dalpe et al. 1999). More specifically, uptake of a low-molecular-weight fluorescent dye (reactive orange 14), to which intact muscle cells are impermeable, was observed for a greater percentage of *dt* diaphragm muscle fibers in comparison to wild-type fibers following a fatigue protocol (Dalpe et al. 1999). This observation suggests that Bpag1 deficiency in skeletal muscle is associated with increased sarcolemmal fragility.

Mice lacking Bpag1 display lower maximum force, delayed recovery of force generation potential, and higher fatigability. These outcomes are hypothesized to be attributable to Bpag1-deficiency which is linked to proposed defects in mitochondrial respiratory function. In this context, mitochondria are known to play an important role in cellular energy production and metabolism, which in turn affects contractile properties.

There is evidence to suggest that the ability of mitochondria to produce energy is affected in part by the cellular localization of these organelles. Although the underlying mechanisms determining the cellular localization of mitochondria are not fully understood, components of the cytoskeleton have been suggested to fulfill this function (Heggeness et al. 1978; Milner et al. 2000). Interestingly, a reported feature of skeletal muscle from Bpag1-deficient mice is the increased clustering of mitochondria at the periphery of muscle fibers, as revealed from ultrastructural studies using electron microscopy (Dalpe et al. 1999). A similar skeletal muscle phenotype has also been reported for desmin-null mice (Milner et al. 2000). Furthermore, in these studies, mitochondrial mis-localization was also associated with mitochondrial dysfunction (Milner et al. 2000). Whether mitochondrial dysfunction resulting from aberrant mitochondrial localization in Bpag1-deficient skeletal muscle occurs, remains an open question.

Desmin IFs are located in the region of the sarcomere, at the level of the Z-discs, where they appear to provide a direct link for mitochondria (Tokuyasu et al. 1983; Milner et al. 1996). Studies on mice lacking desmin show impairments in mitochondrial placement as well as in respiratory function of muscle fibers (Milner et al. 1996; Milner et al. 2000). Given that desmin and Bpag1 expression during myoblast differentiation appears to coincide, it has been postulated that the absence of Bpag1 may lead to abnormal mitochondrial localization by de-stabilizing desmin IFs (Dalpe et al. 1999). It should also be noted that a similar desmin-binding function has been attributed to plectin (Foisner et al. 1995), thereby indicating that plectin and Bpag1 may have overlapping

functions in stabilizing desmin IFs, in turn ensuring proper mitochondrial localization and function .

Impaired localization of mitochondria in skeletal muscle lacking Bpag1 may also be caused by destabilized microtubule networks. In sensory axons, for example, fewer microtubules as well as disorganized microtubule networks and axonal swellings packed with mitochondria have been reported (Bernier and Kothary 1998; Dalpe et al. 1998; Yang et al. 1999). The MTBD found in the C-terminal region of Bpag1 molecules has been shown to stabilize microtubule networks in cultured COS-7 cells (Sun et al. 2001). It is therefore possible that Bpag1 muscle isoforms, which harbor a MTBD within their C-terminus, may stabilize microtubule networks of skeletal muscle thereby contributing to the proper localization of mitochondria.

Why study the role of Bpag1 in skeletal muscle?

Striated muscles are composed of a rich web of interconnected cytoskeletal networks that are essential for the tissues contractile function. More specifically, skeletal muscle cells contain complex arrays of specialized cytoskeletal components making them an ideal cell type for the study of cytoskeletal protein interactions. Skeletal muscle is also easily accessible and processed, making it an ideal tissue for a variety of biochemical, histochemical, and molecular biological approaches. Insights gained from the investigation of skeletal muscle will provide a better understanding as to the function of Bpag1 in other cell types. It is also possible that the functions ascribed to Bpag1

molecules may also provide clues as to the function of other plakin family members sharing sequence similarities with Bpag1. Availability of several mutant mouse models is also advantageous in that they can be studied to gain insights into the normal functions of cytoskeletal proteins. The *dt* mouse model, which will be exploited in the proposed study, is one example.

Statement of the Problem; Hypotheses

It is becoming increasingly clear that Bpag1molecules play a critical role in maintaining the structural integrity of skeletal muscle cells. Which cytoskeletal network of muscle cells (MF, desmin-IF and MT) is dependent on Bpag1 remains to be clearly established. In this context, the primary objective of the present proposed study is to assess the involvement of Bpag1 in the structural integrity of skeletal muscle. Because Bpag1b, the predominant skeletal muscle isoform, harbors an ABD, an IFBD and a MTBD, the distribution of MFs, desmin IFs (skeletal muscle-specific intermediate filament) and MTs may be perturbed in Bpag1-deficient muscle fibers. This implies that changes in the expression of Bpag1, a crosslinking protein, may affect the ability of the primary cytoskeletal networks to function.

We will therefore test the following two primary hypotheses:

1) ***That Bpag1 is involved in directing the cellular localization of muscle cytoskeletal proteins, namely microfilaments, desmin intermediate filaments and microtubules.***

2) ***That <u>the expression levels</u> of muscle cytoskeletal proteins, namely microfilaments, desmin intermediate filaments and microtubules, are affected in skeletal muscle lacking Bpag1.***

Additional elements of the proposed study will aim at determining whether Bpag1-deficiency has a greater impact on slow-twitch fibers versus fast-twitch fibers given that other studies have suggested a higher susceptibility of slow-twitch fibers to cytoskeletal disruptions (as described on page 5).

Materials and Methods

Mice

The dt^{Tg4} line of transgenic mice used for this study was obtained from Dr. Rashmi Kothary from the Ottawa Health Research Institute. Since May 2003, the line has been maintained in the animal care facility at Laurentian University. The mice are housed in wire cages (40 x 25 x 17.5 cm) at room temperature (~ 22°C) with a twelve hour light/dark cycle and are fed mouse chow and water ad libitum. The mice are cared for according to the guidelines of the Canadian Council on Animal Care.

The dt^{Tg4} mouse model was generated inadvertantly when a transgene insertion caused a mutation at the *dt* locus of a CD-1 mouse strain (Kothary et al. 1988) (see Figure 6A). Characterization of the integration site of the transgene led to the identification of Bpag1 as the defective gene (Brown et al. 1995). Homozygous mice display limb incoordination and die 3-4 weeks post-natal of unknown causes.

Genotyping

Isolation of high molecular weight DNA from mouse tails was performed to obtain genomic DNA that was used to conduct PCR-based genotyping to identify wild-type, heterozygous and homozygous mice. In order to do so, 14 day-old mice are euthanized by cervical dislocation. A 1 cm tail clip was collected from each mouse and

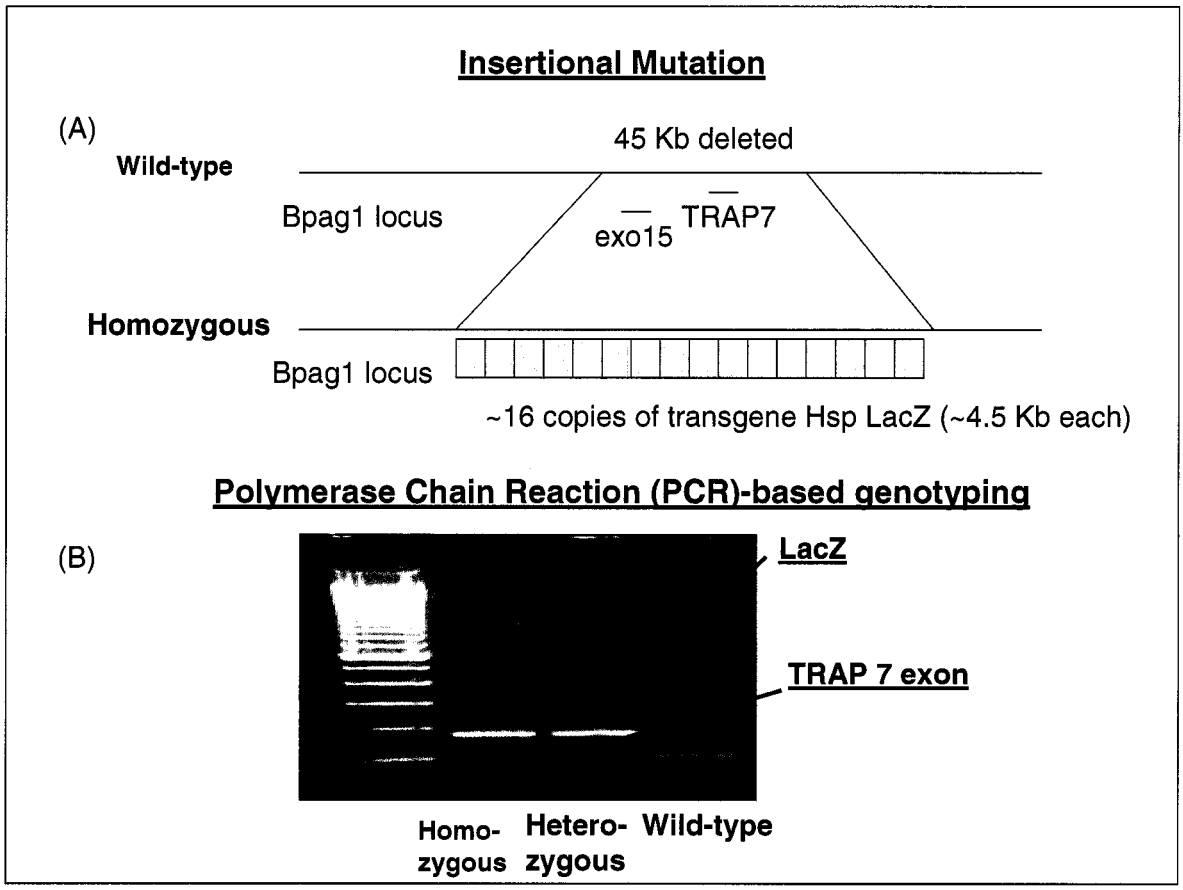

Figure 6 (A) Model of transgene insertion causing a mutation at the Bpag1 locus of a CD-1 mouse strain. (B) Polymerase chain reaction –based genotyping to identify wild-type, heterozygous and homozygous mice.

placed individually into 1.5 ml microtubes either kept on ice or stored at –20°C until further processing. Each tail clip was then digested in 600 uL of Proteinase K buffer (50 mM Tris-HCl pH 8, 100 mM EDTA, 100 mM NaCl, 1% SDS) supplemented with 50 uL of Proteinase K and incubated overnight in a 55-60°C water bath. Once the tails were digested, DNA was isolated using an organic extraction method. Briefly, a phenol chloroform extraction was followed by a choloroform isoamyl alcohol extraction. The aqueous phase was transferred to a clean tube and DNA precipitation was performed using isopropanol. The DNA pellet was then washed with 70% ethanol and air dried before being re-suspended in approximately 50 uL of TE (10 mM Tris-HCl pH7.5, 1 mM EDTA).

Subsequently, the amount of DNA isolated was determined using a spectrophotometer (Beckmann model DV-64). Absorbency values measured at 260 nm using a UV light were collected to determine the DNA concentration. DNA samples at 200 ng/uL were then prepared using TE. These standardized DNA samples were then used to determine the genotype using the polymerase chain reaction (PCR).

Polymerase Chain Reaction (PCR)-based genotyping

Identification of the genotype was performed using two sets of primers (purchased from Alpha DNA, Sherbrooke). The first set (RAS 39, RAS 40: see Table 1) targets the lacZ segment (176 bp) of the mouse transgene, Hsp60-LacZ (Kothary et al. 1988), that is absent in wild-type mice, present on 1 allele in heterozygous mice, and

Table 1. Primer information for Polymerase Chain Reaction (PCR)-based genotyping

Primer Name	Sequence (5' – 3')	Target	PCR product size
RAS 39	TTGGCCTGAACTGCCAGCTGGCGCAGG	LacZ 3931-3957 sense	176 bp
RAS 40	TCCCGCAGCGCAGACCGTTTTCGCTCG	LacZ 4107-4081 anti-sense	
RAS 24	CACCTTGCTGAGGCAGGCTCTCC	TRAP7 sense	94 bp
RAS 22	GATCCTGTGAGACGGGAGAATGT	TRAP7 anti-sense	

present on both alleles in homozygous mice. The second set of primers (RAS 22, RAS 24: see Table 1) targets an exonic region (TRAP7; 94 bp) that is present in the wild-type mice, but deleted on 1 allele of heterozygous mice and deleted in both alleles of homozygous mice (Figure 6B). Genomic DNA (200 ng) was added to a mixture containing 1X PCR buffer, 1X dNTP mixture, primers RAS 22, 24, 39, and 40 (0.2μM each), as well as 1.25 units of Taq DNA polymerase (Invitrogen Molecular Probes, Inc., Eugene, OR). The PCR conditions were as follows: an initial denaturation step at 97°C for 3 minutes was followed by 35 cycles of denaturation at 94°C for 1 minute, annealing at 50°C for 1 minute, and extension at 72°C for 1 minute. In each experiment, the last cycle was followed by a 10 minute elongation step at 72°C. Twenty μL of each PCR sample was loaded onto a 2% ethidium bromide-stained agarose gel (1X TBE). PCR products were resolved for roughly 1 ½ hours at 100 volts. Since wild-type mice do not express the lacZ band, we are able to distinguish them from heterozygous and homozygous mice. Heterozygous mice are distinguished from homozygous mice by the presence of the 94 bp band, corresponding to the exonic region maintained on the non-mutated allele, in heterozygous mice (Figure 6B).

Excision of Hindlimb Skeletal Muscles

Mice were euthanized by cervical dislocation at post-natal day 14. The overlying skin was first cleaned with 70% ethanol. The underlying muscles were exposed by removing the skin. The tissue was kept hydrated using 1X PBS. Next, under a microscope, we carefully removed the connective tissue covering the muscles. With the

mouse lying in a supine position, we performed a blunt dissection of the tibialis anterior, cut the distal tendon at the ankle, and then gently peeled back the muscle and cut the proximal tendon at the knee. The soleus muscles were excised from the hindlimbs by placing the mouse in a prone position. The distal tendon of the soleus muscle was exposed then cut. The muscle was gently peeled and excised by cutting the proximal tendon. Muscles were frozen in pairs (i.e. left and right soleus, left and right tibialis anterior). Tissues destined for protein isolation were flash frozen directly in liquid nitrogen and stored at –80°C in cryovials. Tissues to be processed for immunofluorescence were covered in Histo Prep frozen tissue embedding media (Fisher Scientific International Inc., Hampton, NH) then frozen in isopentane pre-cooled in liquid nitrogen and stored in cryovials at –80°C.

Protein Isolation from Skeletal Muscles

Protein extracts from frozen soleus (approximate weight (mg/pair): wt=3.8, ht=2.2, hm=1.2) and tibialis anterior muscles (approximate weight (mg/pair): wt=17.7, ht=12.4, hm=8.9) were obtained by grinding the frozen tissue with an ice-cold tephlon homogenizer in 750 uL of lysis buffer (150 mM NaCl, 10 mM Tris pH 7.5, 1 mM EDTA pH 7.0, 1 mM EGTA pH 9.0, 50 mM NaF, 1 % Triton-X, 1 mM Vanadate pH 10) containing protease inhibitors (1 µg/ml Leupeptin, 1 µg/ml Aprotinin, 5µg/ml PMSF). The resulting samples were then centrifuged at 4500 RCF, for 1 hour at 4°C.

The protein concentrations were subsequently measured using the Bradford reaction. Briefly, protein samples (made with Bovine Serum Albumine - BSA) of varying concentrations were prepared with the Bradford reagent (BR) and their absorbency readings at a wavelength of 595 nm were measured with a spectrophotometer to create a standard curve. The soleus and tibialis anterior –derived protein lysates were prepared for the Bradford assay and their concentrations were derived from the standard curve. Protein lysates were stored in small aliquots at -80°C to avoid repeated cycles of freeze thawing.

SDS-Polyacrylamide Gel Electrophoresis (SDS-PAGE)

Loading buffer (60 mM Tris pH 6.8, 2% SDS, 10% Glycerol, 5% beta-mercaptoethanol pH 6.8, 0.4% Bromophenol) was added to 10 µg samples of soleus and tibialis anterior protein lysates. Protein samples were then heated at 100°C for 5 minutes then placed on ice. Subsequently, protein samples were loaded on a 5% stacking gel (5% acrylamide mix, 125 mM Tris pH 6.8, 0.05% SDS, 0.1% ammonium persulfate, 0.001 µl/ml TEMED) and resolved on a 10% acrylamide gel (10% acrylamide mix, 375 mM Tris pH 8.8, 0.05% SDS, 0.1% ammonium persulfate, 0.0001 µl/ml TEMED) for approximately 1 hour at 200 Volts in 1X Running buffer (25 mM Tris base, 250 mM Glycine pH 8.3, 0.1% SDS).

Semi-Dry Transfer of Proteins from Polyacrylamide Gel to a Polyvinylidene Fluoride Microporous (PVDF) Membrane

Once proteins were resolved, the gel was placed in cathode buffer (0.3 M Tris base, 20% MeOH) for 15 minutes. During this time, we processed the PVDF membrane as follows: 1) incubation in 100% methanol for 15 seconds, 2) incubation in H_20 for 2 minutes, 3) incubation in anode II buffer (0.025 M Tris base, 20% MeOH) for 10 minutes. Next, we prepared a sandwich made up of 3 sheets of Whatman 3 MM filter papers soaked in cathode buffer, 1 gel, 1 PVDF membrane, 1 filter paper soaked in anode II buffer, and 2 filter papers soaked in anode I buffer (0.025 M Tris base). The transfer was usually performed for 20 minutes at 0.22 AMPS (2.5 mA/cm^2).

Immunodetection of Desmin, Tubulin and Actin

Once the protein transfer was complete, the membrane was placed in a blocking buffer (5% non-fat dried milk in 1X TBST made of 0.02 M Tris base, 0.1 M NaCl, 0.002 M KCl, 0.1% Tween) overnight at 4°C, in order to reduce the extent of non-specific binding of the primary antibodies. The membrane was then probed for either desmin, actin, or tubulin (separate membranes were used for each of the proteins examined) using mouse monoclonal anti-desmin, mouse monoclonal anti-actin, and mouse monoclonal anti-α-tubulin primary antibodies respectively (Sigma Chem. Co., St. Louis, MO). The antibodies were diluted (Table 2) in blocking buffer and the membrane was added to the liquid then sealed in a bag and put on an orbital shaker for 1 hour. We then performed 4

Table 2. Primary and secondary antibodies used for immunodetection

Antibody	**Dilution Western(W)/ Immunofluorescence (I)**	**Purchased from**
mouse monoclonal anti-desmin primary antibody	(W) 1 : 400 (I) 1 : 20	Sigma Chem.
mouse monoclonal anti-α-actin primary antibody	(W) 1 : 1000	Sigma Chem.
mouse monoclonal anti-α-tubulin primary antibody	(W) 1 : 1000 (I) 1 : 1000	Sigma Chem.
goat anti-mouse horseradish peroxidase (HRP) conjugate secondary antibody	(W) 1 : 5000	Invitrogen Molecular Probes
goat anti-mouse fluorochrome-conjugated secondary antibody Alexa Fluor 488	(I) 1 : 800	Invitrogen Molecular Probes
Hoechst bis-benzimide	(I) 1 : 5000	Sigma Chem.
Rhodamine conjugated phalloidin	(I) 1 : 400	Invitrogen Molecular Probes
mouse monoclonal anti-myosin heavy chain I (MHC I) primary antibody	(I) 1 : 1000	Invitrogen Molecular Probes

washes on an orbital shaker by placing the membrane in 300 ml of 1X TBST for 10 minutes per wash. Once the first set of washes was complete, secondary detection of the primary antibodies was performed by placing the membrane in a solution containing 1X TBST and goat anti-mouse horseradish peroxidase (HRP) conjugated secondary antibody (Invitrogen Molecular Probes, Inc., Eugene, OR). The membrane was incubated with the secondary antibody for 1 hour on an orbital shaker and was subsequently washed in 1X TBST four times. After the wash cycle, the secondary antibody was detected using the Enhanced chemiluminescent (ECL) kit (Amersham Corp., Arlington Heights, IL). The membrane was then processed for autoradiography. Images were also collected using a Bio-Rad gel documentation system (Bio-Rad Laboratories Ltd., Canada).

Densitometric Analysis

Images collected with the gel documentation system were analyzed using the Quantity One program (Bio-Rad Laboratories Ltd., Canada). The program uses light detectors to convert signals from biological samples into digital data. Each protein band was circled separately then quantified by subtracting the background from the overall density of the sample (Figure 7). Although the amount of total protein loaded onto the gel was equal (10 μg each sample), an additional verification step was performed to ascertain that the transfer process from the gel to the membrane was uniformly efficient. Membranes were therefore stained with the EZBlue gel staining reagent (Sigma Chem. Co., St. Louis, MO) which stains all proteins. The membrane was then re-scanned with the gel documentation system and the Quantity One program was used to determine the

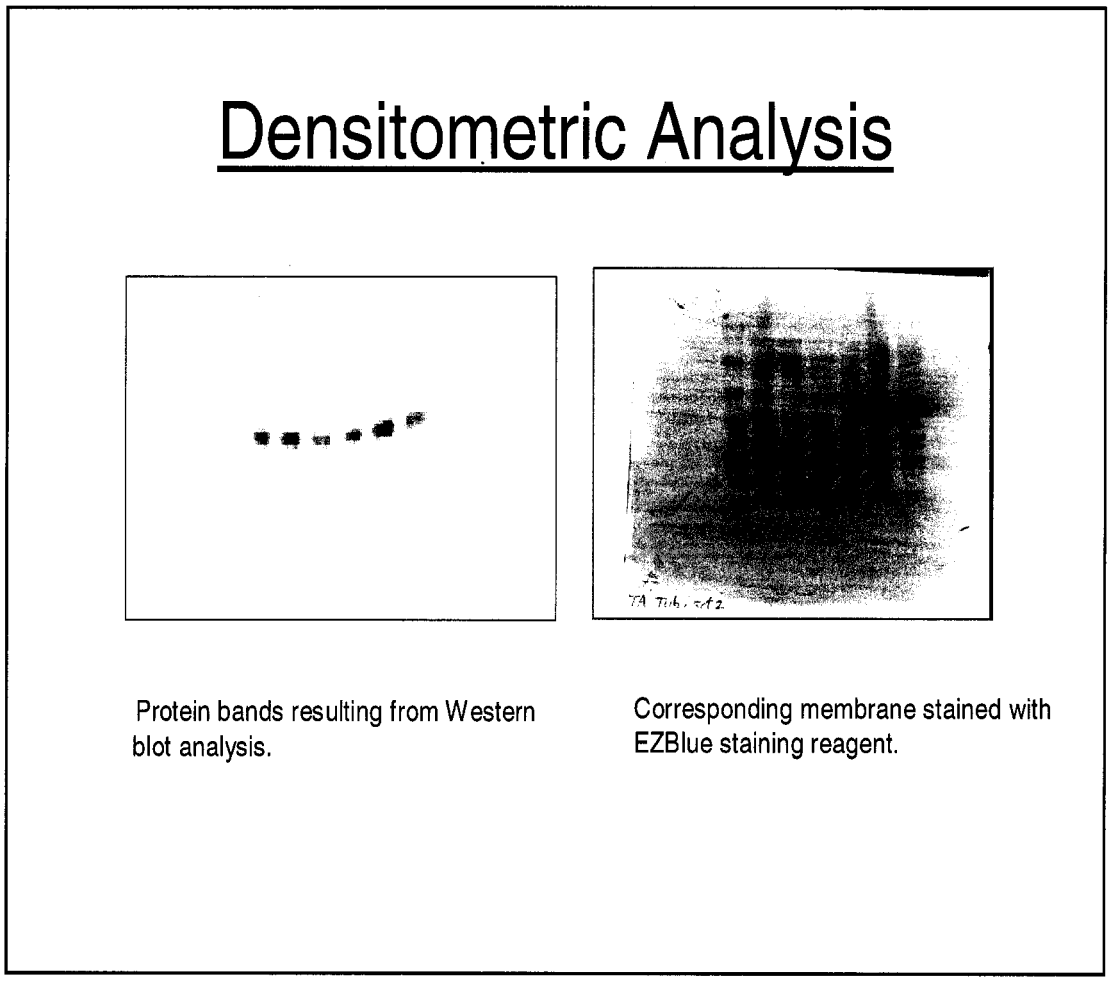

Figure 7 Images are examples of protein bands from Western blot analysis and corresponding membrane stained with EZBlue staining reagent used to quantify cytoskeletal protein levels.

total amount of protein per lane. These values were used as internal controls to standardize the levels of desmin, α-actin, and α-tubulin.

Collecting Skeletal Muscle Tissue Sections Using a Cryostat

Frozen soleus and tibialis anterior tissues kept at -80°C were placed at -20°C for 30 minutes before sectioning. Samples were then mounted on a "chuck" using Histo Prep compound and sectioned longitudinally at a thickness of 10 μm using a cryostat (model CM3050, Leica Microsystems Inc., Canada). Serial sections were collected on microscope slides (Superfrost Plus, Fisher Scientific International Inc., Hampton, NH) then stored at -80°C until further processing.

Immunofluorescence

Muscle sections were first brought to room temperature in a moist chamber. Next, sections were fixed using 4% paraformaldehyde (PFA) for 10 minutes. Fixing tissues preserves tissue integrity. After soaking slides in 1X PBS twice for 5 minutes, tissue sections were incubated in a blocking/permeabilizing solution (5% Horse-serum and buffer A containing 1X PBS, 0.15% glycine and 0.5% BSA) for 15 minutes. The sections were then incubated with primary antibodies targeting either desmin or α-tubulin (Table 2) diluted in buffer A for 1 hour in the dark. The tissue sections were then rinsed 3 times for 15 minutes with buffer A. Secondary detection of the primary antibodies was performed for 1 hour in the dark by incubating slides with a goat anti-mouse

fluorochrome (Alexa Fluor 488)-conjugated secondary antibody (Invitrogen Molecular Probes, Inc., Eugene, OR) diluted in buffer A (Table 2). Nuclei were detected using Hoechst bis-benzimide (Sigma Chem. Co., St. Louis, MO) and F-actin microfilaments were visualized using rhodamine conjugated phalloidin (Invitrogen Molecular Probes, Inc., Eugene, OR). Type I slow-twitch fibers were distinguished from type II fast-twitch fibers using a mouse monoclonal anti-myosin heavy chain I (MHC I) primary antibody. The sections were then rinsed 3 more times for 15 minutes in 1X PBS, then mounted in GelTol aqueous mounting medium (Thermo Electron Shandon products, Sigma Chem. Co., St. Louis, MO) and kept at room temperature in the dark. Sections were visualized using the Zeiss Axiovert 200M fluorescent inverted deconvolution microscope and images were acquired using an AxioCam HR camera and the Axio Vision 4.2 computer software program.

Statistical Analysis

Protein expression levels (dependent variable 1) were compared according to genotype (independent variable 1: homozygous versus heterozygous versus wild-type) and fiber type (independent variable 2: slow-twitch versus fast-twitch) using multivariate (MANOVA; 1 factor analysis according to genotype due to a lack of subjects) and univariate (ANOVA; 1 factor analysis of genotype according to respective fiber-type) analysis of variance respectively. Significance was set at $P<0.05$. In order to ensure non biased sample analysis of immunofluorescence images, a blind analysis (scrambled images) was performed using specific staining patterns as the main criteria for

cytoskeletal organization. For wild-type skeletal muscle, desmin staining was expected throughout the cytoplasm, specifically localized at the Z-lines, α-actin staining was expected throughout the entire fiber's cytoplasmic region, whereas α-tubulin staining was anticipated to be within perinuclear and subsarcolemmal regions. The frequency of fibers displaying these staining patterns (dependent variable 2) was then analyzed according to genotype and fiber type using loglinear analysis (2 factor analysis). Significance was set at $Z \geq 1.96$.

Results

Given that Bpag1 harbors binding sites for the primary components of the cytoskeleton (MFs, IFs and MTs), it is argued that Bpag1 proteins interact with MFs, IFs and MTs thereby integrating the functions of these cytoskeletal networks (Leung et al. 2002). Accordingly, in the present study, the impact of Bpag1-deficiency on the expression levels of MF, IF and MT subunits, and the subcellular localization of these cytoskeletal elements was assessed in skeletal muscle.

Body Mass According to Genotype

Overall size and body mass of 14 days post-natal wild-type, heterozygous and homozygous mice from the dt^{Tg4} line were documented (Appendix 1). Wild-type and heterozygous mice have nearly identical body mass, whereas homozygous mice are approximately 30% lighter than wild-type and heterozygous littermates which is likely the result of disuse atrophy ($p<0.05$) (Figure 8).

The Impact of Bpag1-deficiency on the Expression Levels of Desmin, α-Tubulin and α-Actin

1) Overall Protein Expression Levels

Bpag1b isoforms (b1, b2) are the predominant isoforms expressed in contractile tissue (Leung et al. 2001). These isoforms are thought to interact with MFs, IFs and MTs

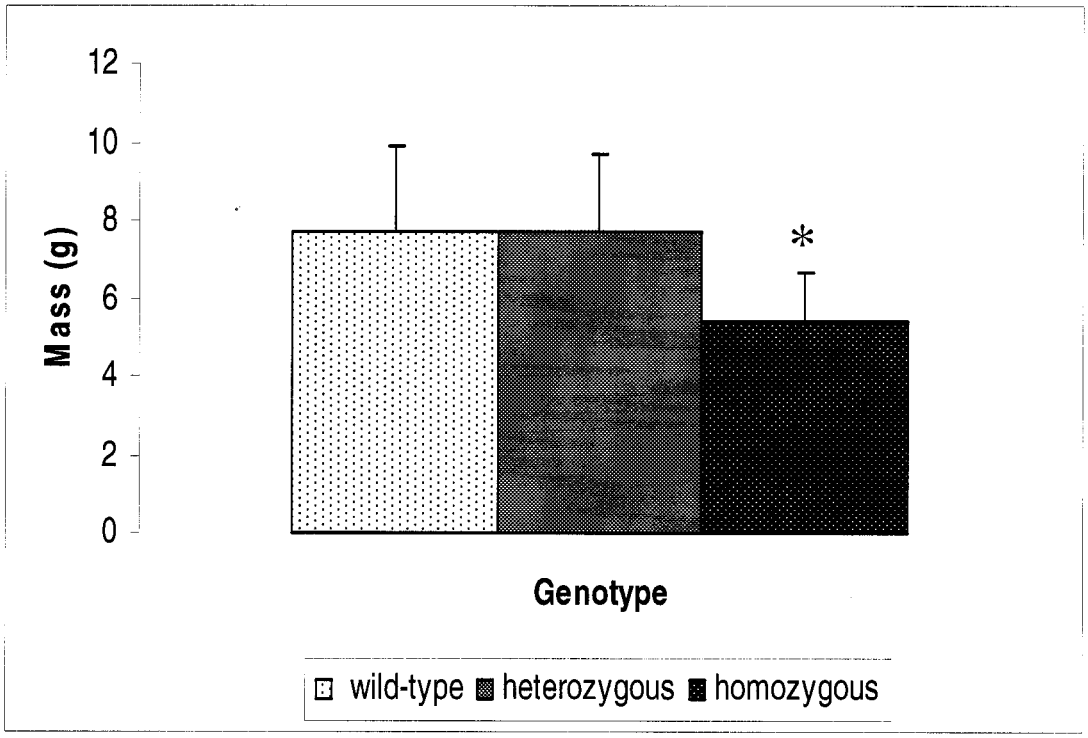

Figure 8 Comparison of mean body mass between wild-type, heterozygous and homozygous mice. *Denotes significant differences from wild-type and heterozygous ($p<0.05$).

given that they harbor specific interaction domains for each of these cytoskeletal elements. We therefore hypothesized that these specific cytoskeletal proteins would be affected in the absence of Bpag1 molecules. To address this issue, we performed Western blot analyses using total protein isolated from the soleus and tibialis anterior muscles of wild-type, heterozygous and homozygous mice, and using antibodies specific to α-actin, desmin and α-tubulin (Table 2). Multivariate analysis of overall mean protein expression levels of the targeted molecules (i.e. α-actin, desmin, α-tubulin) demonstrates that, regardless of muscle type, there is a significant difference in the amount of proteins according to genotype ($p<0.05$). More specifically, using wild-type values as the baseline for comparison, the overall levels of target protein expressed in skeletal muscle from homozygous mice are approximately 73% of wild-type values (100%), for α-actin, desmin and α-tubulin combined ($p<0.05$), whereas values obtained from skeletal muscle of heterozygous mice (93% of wild-type value) were comparable to those of wild-type littermates ($p>0.05$) (Figure 9). Additional statistical analyses were performed using univariate analysis of variance (one way ANOVA) in order to compare the specific expression levels of α-actin, desmin and α-tubulin, individually, across genotypes.

2) Desmin protein expression levels

Desmin IFs are the predominant IF expressed in striated muscle (Lazarides 1980). Furthermore, previous lines of evidence suggest an association between desmin and the IFBD1 of Bpag1 *in vitro* (Dalpe et al. 1999). We therefore anticipated that Bpag1-deficiency would have an impact on the levels of desmin protein in skeletal muscle.

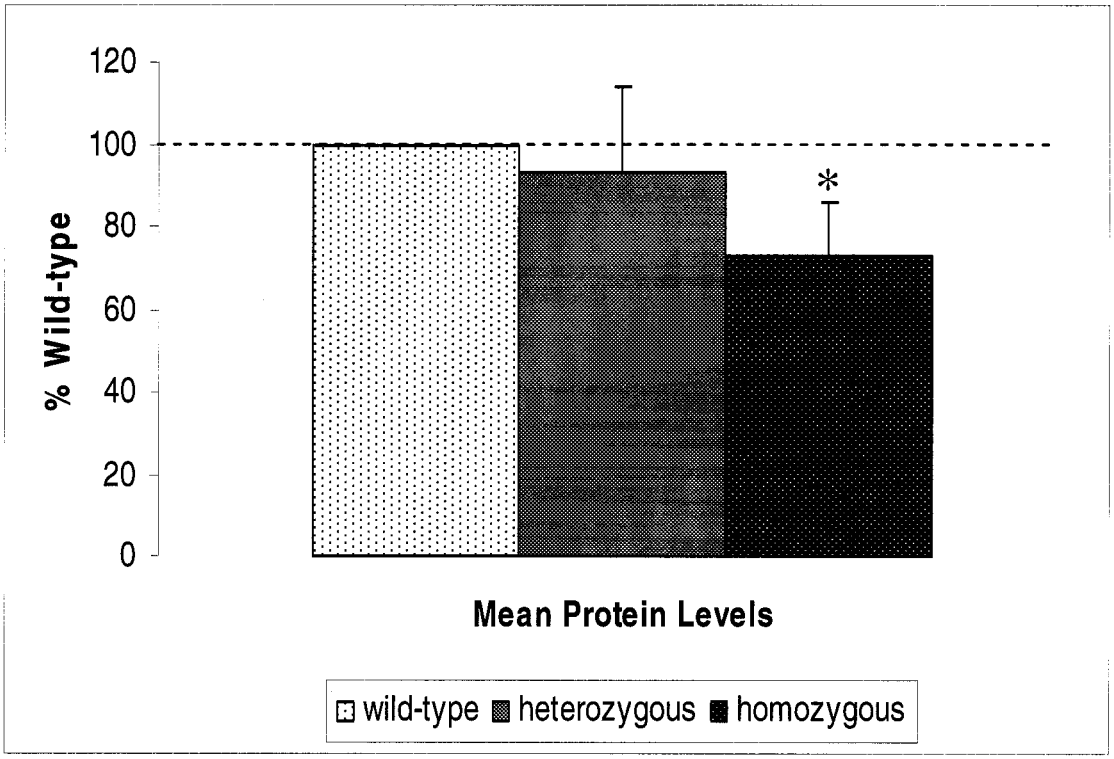

Figure 9 Graph representing overall protein expression levels of the targeted cytoskeletal proteins (desmin, α-tubulin and α-actin) in skeletal muscle from heterozygous and homozygous mice as determined by Western blot analyses. Values are % means ± standard deviation. *Denotes significant differences from wild-type (set at 100%) ($p<0.05$).

Western blot analyses revealed that desmin protein levels remain largely unaffected in muscle from either heterozygous (76%) or homozygous (86%) mice when compared to wild-type littermates, according to multivariate analysis of variance; $p>0.05$ (Figure 10). This observation was also made for both predominantly slow- and fast-twitch skeletal muscle (ANOVA, $p>0.05$).

3) Tubulin Protein Expression Levels

MTs are known for providing strength to the muscle cytoskeleton. Using transfected COS-7 cells, the MTBD of Bpag1 molecules has been shown *in vitro* to stabilize the MT network by binding to microtubules (Sun et al. 2001). We therefore assessed whether tubulin protein levels would be negatively affected in the absence of Bpag1. Western blot analyses of α-tubulin protein levels revealed a significant reduction in the levels of α-tubulin in the slow-twitch muscle of homozygous *dt* mice (54% of wild-type value; ANOVA, $p<0.05$), whereas α-tubulin levels in slow-twitch muscles from heterozygous mice (86% of wild-type value) were comparable to those of wild-type muscle ($p>0.05$) (Figure 11). Levels of α-tubulin in fast-twitch muscle were not affected in either heterozygous (93% of wild-type value) or homozygous (73% of wild-type value) mice, as demonstrated by univariate analysis of variance ($p>0.05$).

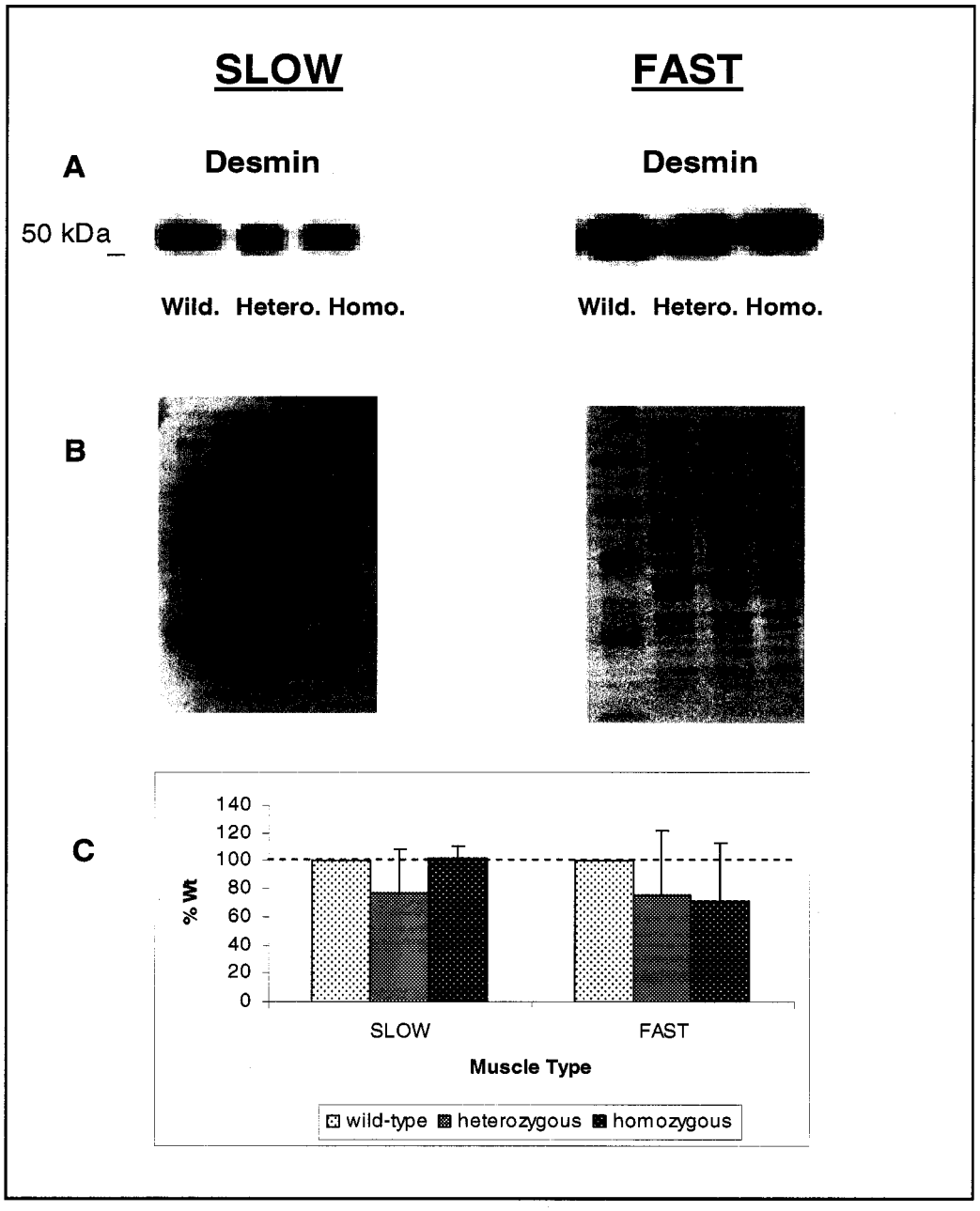

Figure 10 Impact of Bpag1-deficiency on desmin protein levels as determined by Western blot analysis. (A) Representative SDS-PAGE Western blots showing desmin protein levels in slow-twitch (SLOW) and fast-twitch (FAST) muscles from wild-type, heterozygous and homozygous mice. (B) Corresponding coomassie-stained membrane demonstrating equal loading of protein (lane 1 is the ladder). (C) Densitometric analysis of Western blots. Band densities were determined by image analysis and normalized to the sum of the band densities from the coomassie-stained membrane then compared to wild-type protein levels. Values are percent means ± standard deviation. No significant differences were found according to genotype or fiber type ($p>0.05$).

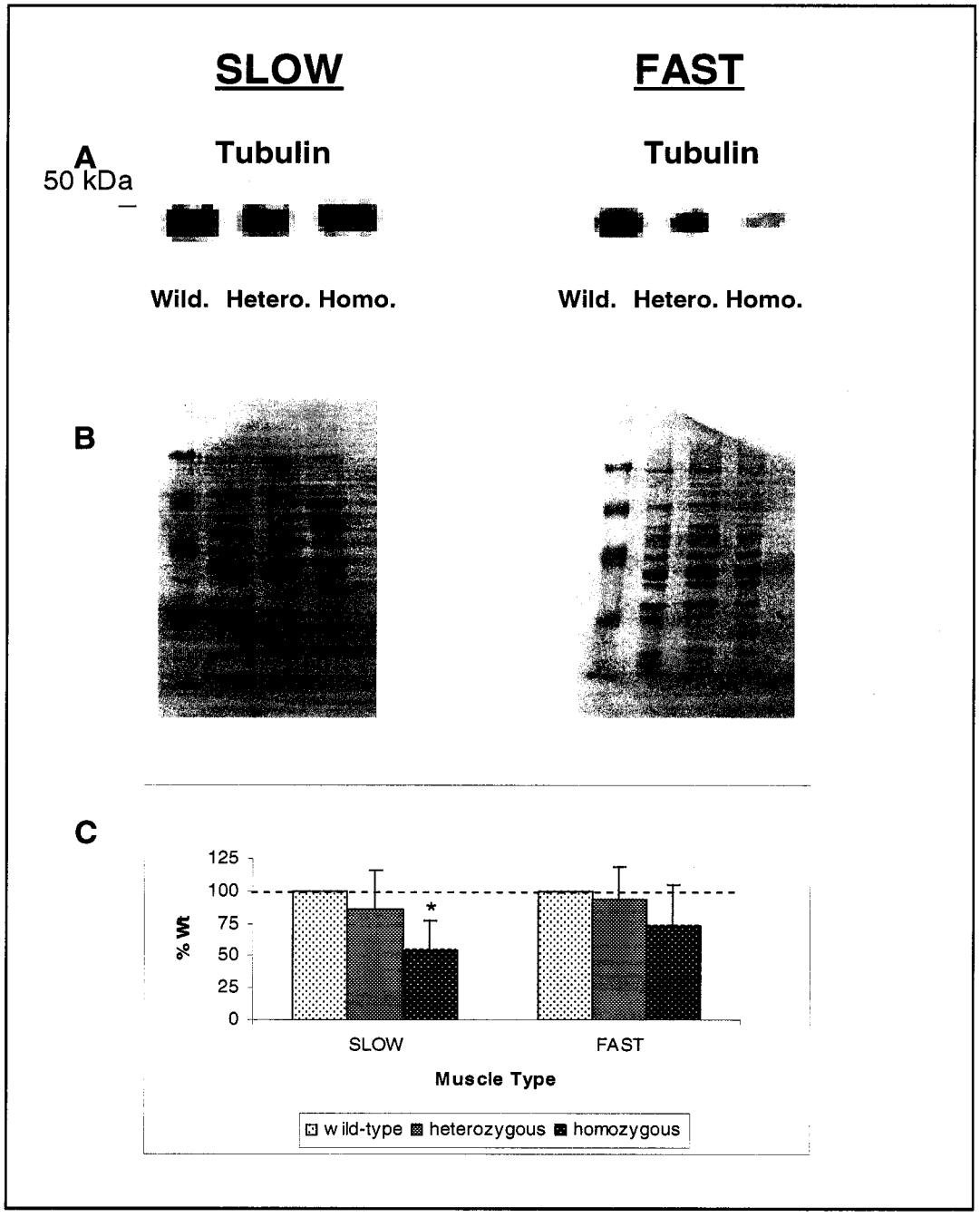

Figure 11 Impact of Bpag1-deficiency on α-tubulin protein levels as determined by Western blot analysis. (A) Representative SDS-PAGE Western blots showing α-tubulin protein levels in slow-twitch (SLOW) and fast-twitch (FAST) muscles from wild-type, heterozygous and homozygous mice. (B) Corresponding coomassie-stained membrane demonstrating equal loading of protein (lane 1 is the ladder). (C) Densitometric analysis of Western blots. Band densities were determined by image analysis and normalized to the sum of the band densities from the coomassie-stained membrane then compared to wild-type protein levels. Values are percent means ± standard deviation. *Denotes significant differences from wild-type (100%) ($p<0.05$).

4) Actin Protein Expression Levels

Actin binding assays using polymerized actin and fusion proteins containing the ABD of Bpag1, have revealed a high level as well as a specific degree of association between MFs and the ABD (Yang et al. 1996). Given the association between Bpag1 and actin microfilaments and their apparent co-localization in C2C12 myogenic cells (Dalpe et al. 1999), the expression levels of α-actin may be affected in homozygous *dt* mice. Western blot analyses of α-actin protein levels in both slow-twitch and fast-twitch muscle revealed a significant difference in α-actin expression levels ($p<0.05$) (Figure 12). More specifically, muscles from homozygous mice express significantly less α-actin (SLOW 61%; FAST 60%, $p<0.05$) compared to wild-type muscle (100%), whereas muscles from heterozygous mice (SLOW 125%; FAST 107%, $p>0.05$) express similar levels as those reported for wild-type muscle.

The Impact of Bpag1-deficiency on the Cellular Localization of IFs, MTs and MFs in Muscle

In cultured cells, IF (neurofilaments) and actin networks have been shown to be restructured in the presence of Bpag1 molecules harboring both the ABD and the IFBD1 resulting in the co-localization of Bpag1, actin MFs and IFs as revealed by immunofluorescence staining (Yang et al. 1996). Given that Bpag1-b (the predominant isoform found in skeletal muscle) harbors an ABD, an IFBD and a MTBD, it was hypothesized that the absence of this gigantic crosslinking molecule would restructure the

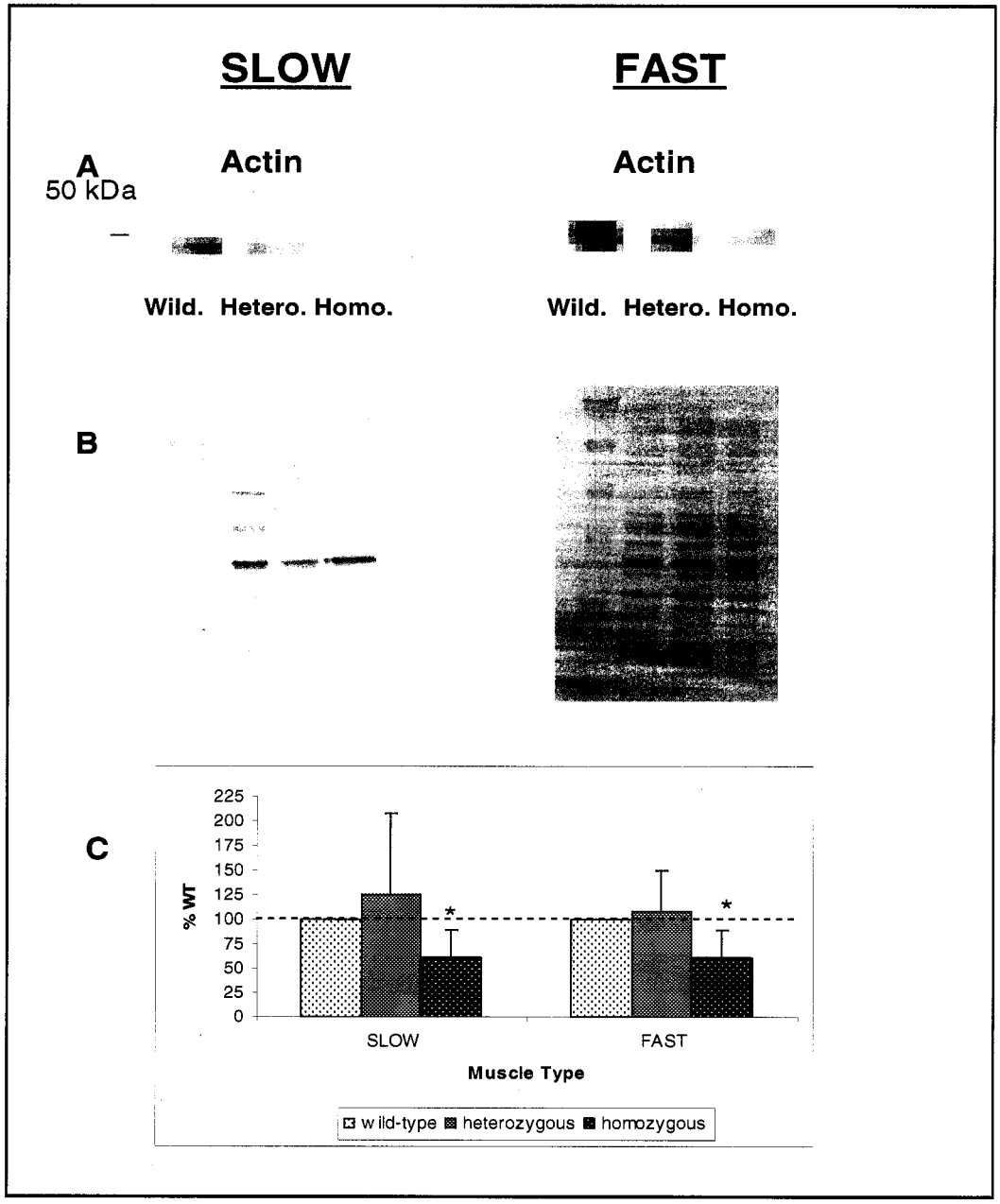

Figure 12 Impact of Bpag1-deficiency on α-actin protein levels as determined by Western blot analysis. (A) Representative SDS-PAGE Western blots showing α-actin protein levels in slow-twitch (SLOW) and fast-twitch (FAST) muscles from wild-type, heterozygous and homozygous mice. (B) Corresponding coomassie-stained membrane demonstrating equal loading of protein (lane 1 is the ladder). (C) Densitometric analysis of Western blots. Band densities were determined by image analysis and normalized to the sum of the band densities from the coomassie-stained membrane then compared to wild-type protein levels. Values are percent means ± standard deviation. *Denotes significant differences from wild-type (100%) ($p<0.05$).

MF, MT and desmin IF networks in skeletal muscle. To test this hypothesis, the subcellular localization of MFs, MTs and desmin was assessed by performing immunofluorescence experiments using longitudinal sections of tibialis anterior muscles from wild-type (n=4), heterozygous (n=4) and homozygous *dt* (n=4) mice and antibodies targeting α-tubulin and desmin, as well as fluorescently tagged phalloidin to detect F-actin (Table 2). Control experiments were performed to evaluate the levels of background fluorescence detected with either primary antibodies targeting desmin or α-tubulin or the Alexa 488-conjugated secondary antibody (Figure 13). Fluorescence was not detected from muscle sections exposed to either desmin (Figure 13A) or tubulin (Figure 13B) antibodies without subsequent secondary detection using the Alexa 488-conjugated secondary antibody. Similarly, minimal fluorescence was detected from muscle sections exposed to the Alexa 488-conjugated secondary antibody without prior exposure to either desmin or tubulin primary antibodies (Figure 13C).

1) Desmin Clumping and Reduced Z-line Staining in Bpag1-deficient Muscle Fibers

Desmin is a component of the Z-line, costameres, and myotendinous junction of skeletal muscle (Lazarides 1980). In the present study, similar desmin staining patterns were observed for wild-type and heterozygous mice in the form of intense desmin staining around the Z-lines, throughout the entire skeletal muscle fiber (Figure 14 A & C). Compared to wild-type and heterozygous mice, desmin appears to be aberrantly localized in skeletal muscle fibers from homozygous *dt* mice. Immunofluorescence images reveal a lack of desmin staining at the Z-lines for a large portion of the muscle

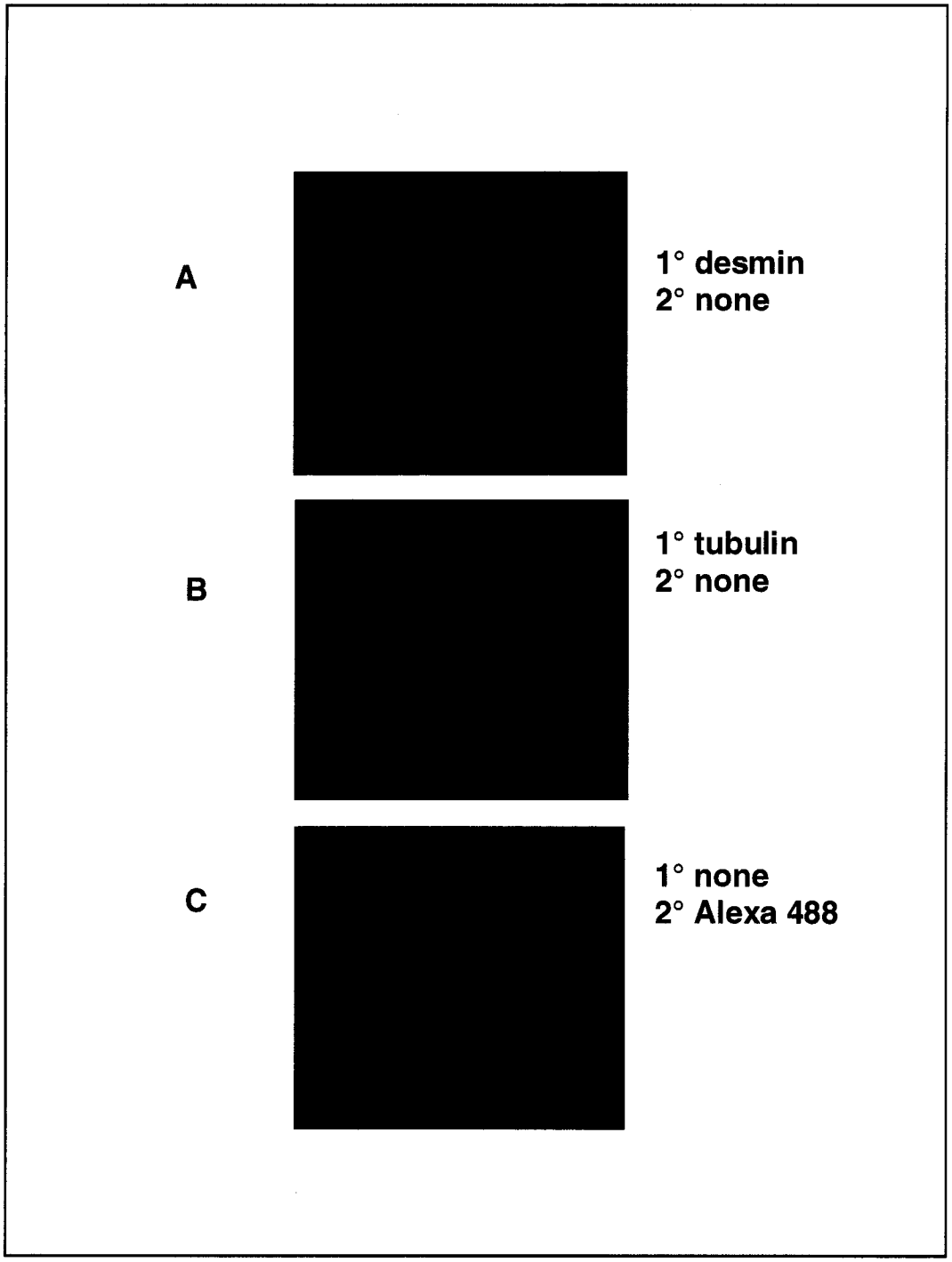

Figure 13 Shown are longitudinal sections of tibialis anterior muscle from wild-type mice stained with (A) anti-desmin and Hoechst, but with no secondary antibody, (B) anti-α-tubulin and Hoechst, but with no secondary antibody and (C) Alexa Fluor 488-conjugated secondary antibody without prior exposure to primary antibodies. A and B are overlayed images collected using FITC and DAPI channels. C is an image collected using the FITC channel.

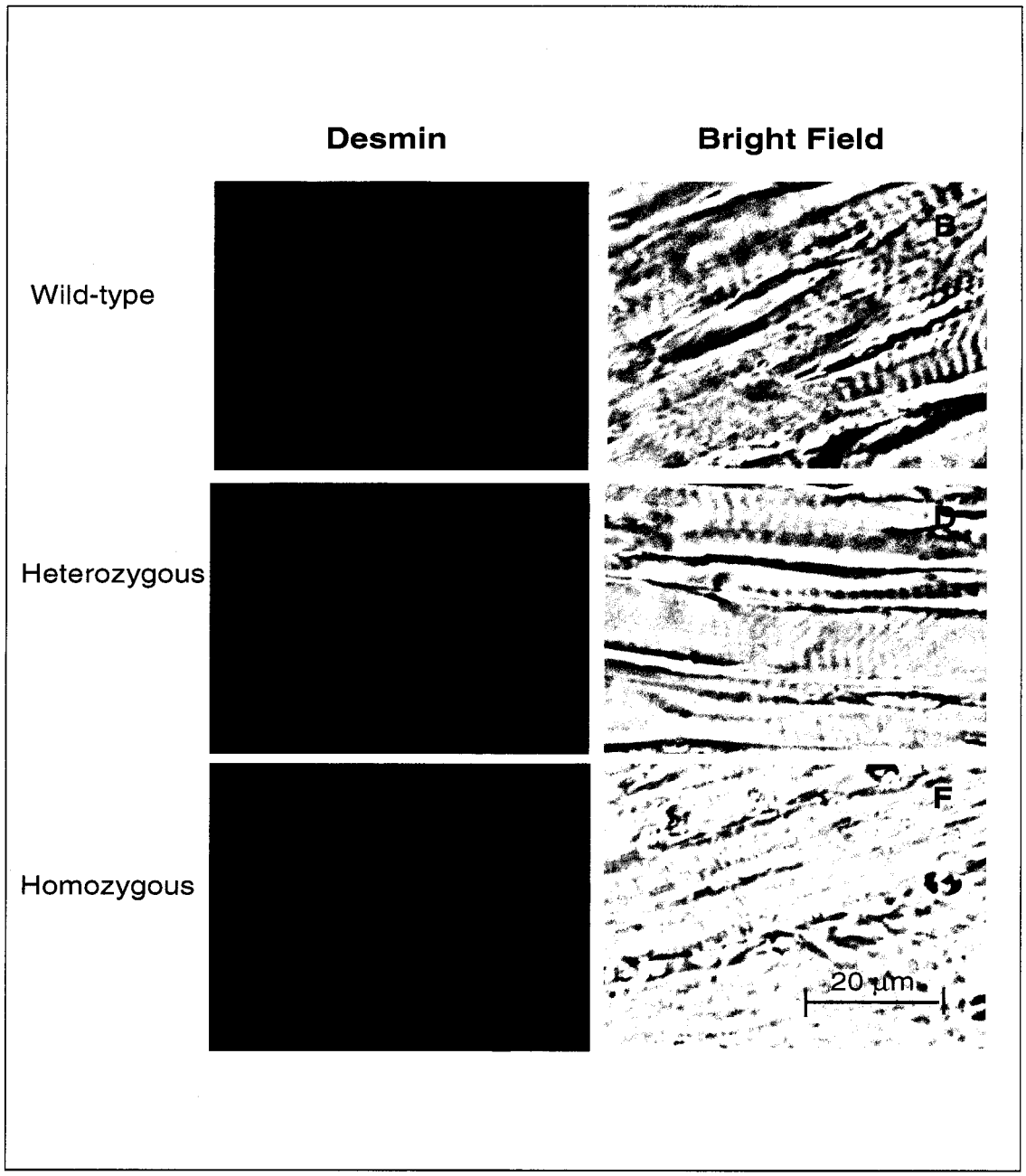

Figure 14 Fluorescence of the cytoskeletal protein desmin (green) in longitudinal sections of tibialis anterior muscle from wild-type (A), heterozygous (C) and homozygous (E) mice. Nuclei are shown in blue (Hoechst). Striations are evident in the bright field images (B, D, F), but desmin immuno-reactive product, specifically localized at striations (arrow 1), is observed for wild-type and heterozygous mice only (A, C). Approximately 71% of fibers from homozygous mice displayed desmin clumping (arrow 2) and lack of Z-line staining (E) ($z>1.96$).

fibers analyzed. The staining pattern appears to indicate clumping of IFs along the subsarcolemmal and cytoplasmic regions (Figure 14E). The staining pattern of over 115 muscle fibers was analyzed for wild-type (n=117), heterozygous (n=162) and homozygous *dt* (n=137) samples from a total of 4 mice for each genotype (see Appendix B). Furthermore, the staining pattern for slow-twitch and fast-twitch muscle fibers was monitored. Slow-twitch fibers were distinguished from fast-twitch fibers by staining serial sections of muscle with a myosin heavy chain (MHC I) antibody that targets myosin Heavy Chain I expressed specifically in slow-twitch muscle fibers (see Figure 15 for example). Loglinear analysis was performed in order to assess the frequency of muscle fibers displaying a normal desmin staining pattern for each genotype. The analyses reveal a high frequency of homozygous muscle fibers (71%) displaying abnormal desmin staining patterns (z=+2.8). Furthermore, the prevalence of desmin disorganization was found to be similar for slow- and fast-twitch muscle fibers. Thus, the absence of Bpag1 has resulted in desmin cytoskeletal disorganization in the form of clumping and a loss of Z-line staining as evidenced by immunofluorescence experiments (Figure 16).

2) Tubulin Cytoskeleton is Perturbed in Bpag1-deficient Muscle Fibers

In skeletal muscle, MTs are positioned between myofibrils and are also associated with nuclei, the Golgi complex and the sub-sarcolemmal region (Ralston et al. 1999; Clark et al. 2002). In the presence of Bpag1, MT staining is faint throughout the muscle

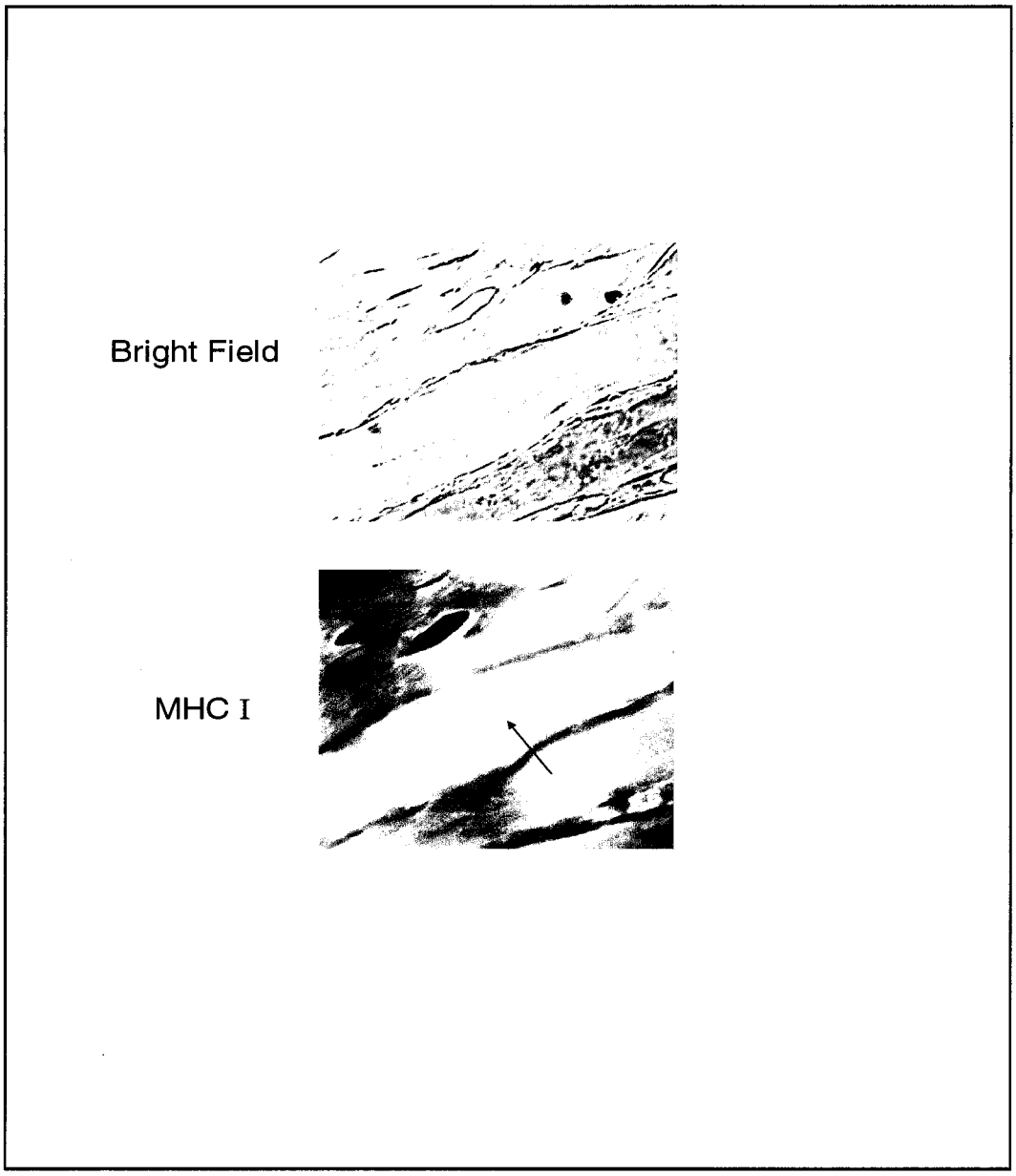

Figure 15 Identification of slow-twitch muscle fibers in serial sections of tibialis anterior muscles. Slow-twitch fiber (arrow) stained with the primary antibody targeting myosin heavy chain 1 (MHC I) and detected using Alexa Fluor 488-conjugated secondary antibody.

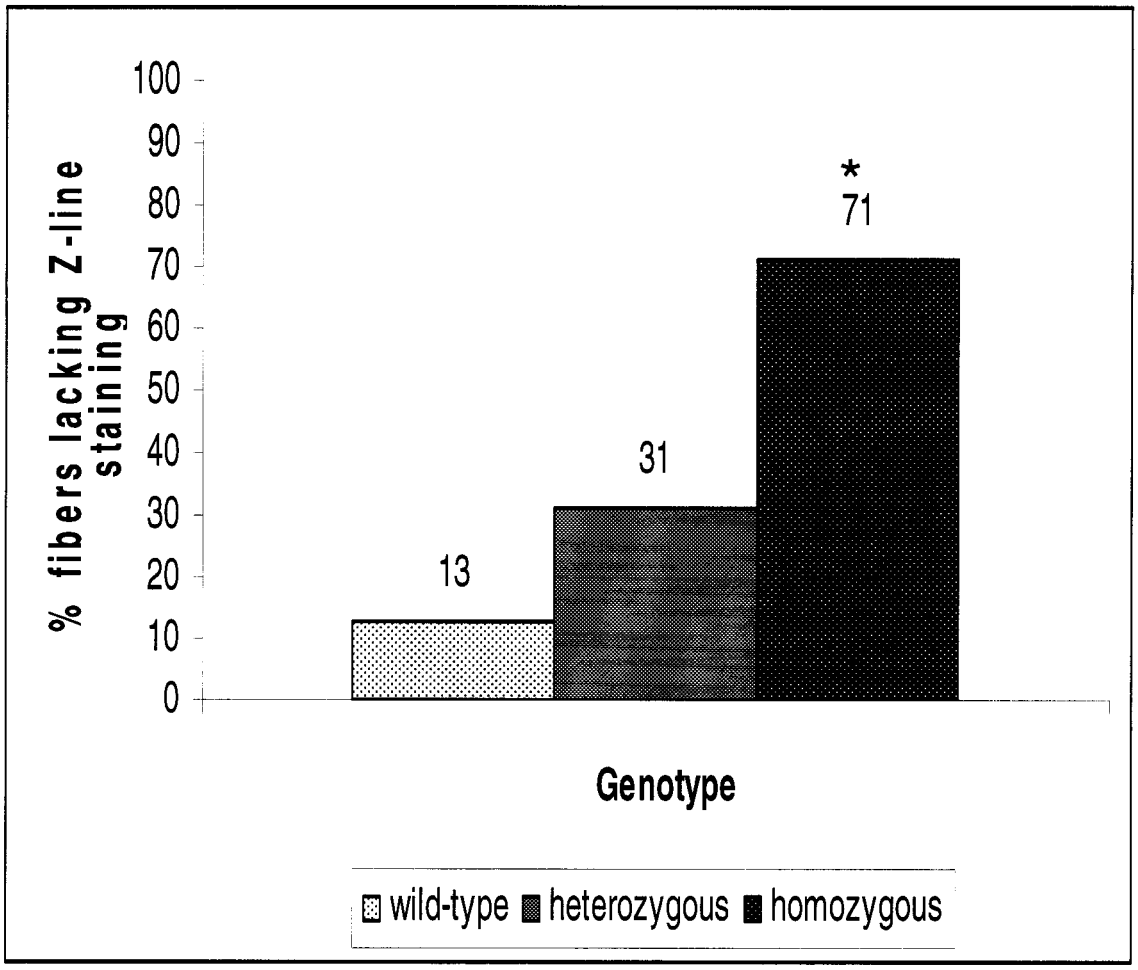

Figure 16 Loglinear analysis results. Observed frequency of muscle fibers displaying a lack of desmin staining at Z-lines. *Denotes significant difference according to genotype ($z>1.96$).

fiber's cytoplasm with more intense staining within the subsarcolemmal region and within the peri-nuclear regions (Figure 17). Immunofluorescence staining experiments of homozygous Bpag1-deficient muscle, reveal uneven staining throughout the cytoplasm, as well as minimal staining within the subsarcolemmal region of muscle fibers. The staining pattern of over 95 muscle fibers was analyzed for wild-type (n=128), heterozygous (n=127) and homozygous (n=97) muscle samples from a total of 4 mice for each genotype (Figure 18). Furthermore, the staining pattern for slow-twitch and fast-twitch fibers was monitored. Loglinear analysis was performed in order to assess and compare the observed frequency of muscle fibers displaying aberrant tubulin localization. The analyses reveal an elevated frequency of homozygous muscle fibers (52%) displaying abnormal tubulin staining as previously described (z=3.9). This observation applies to both slow- and fast-twitch muscle fibers. Thus, the absence of Bpag1 has resulted in tubulin cytoskeletal disorganization in the form of uneven staining patterns and a loss of sub-sarcolemmal staining as evidenced by immunofluorescence experiments.

3) Actin is Aberrantly Localized in Bpag1-deficient Muscle Fibers

Multiple actin isoforms are synthesized in skeletal muscle and can be classified as sarcomeric (found within the sarcomere) or exosarcomeric/cytoplasmic (found outside the sarcomere). Skeletal muscle from wild-type and heterozygous mice displayed an intense even staining for actin throughout the cytoplasm and sub-sarcolemmal region of

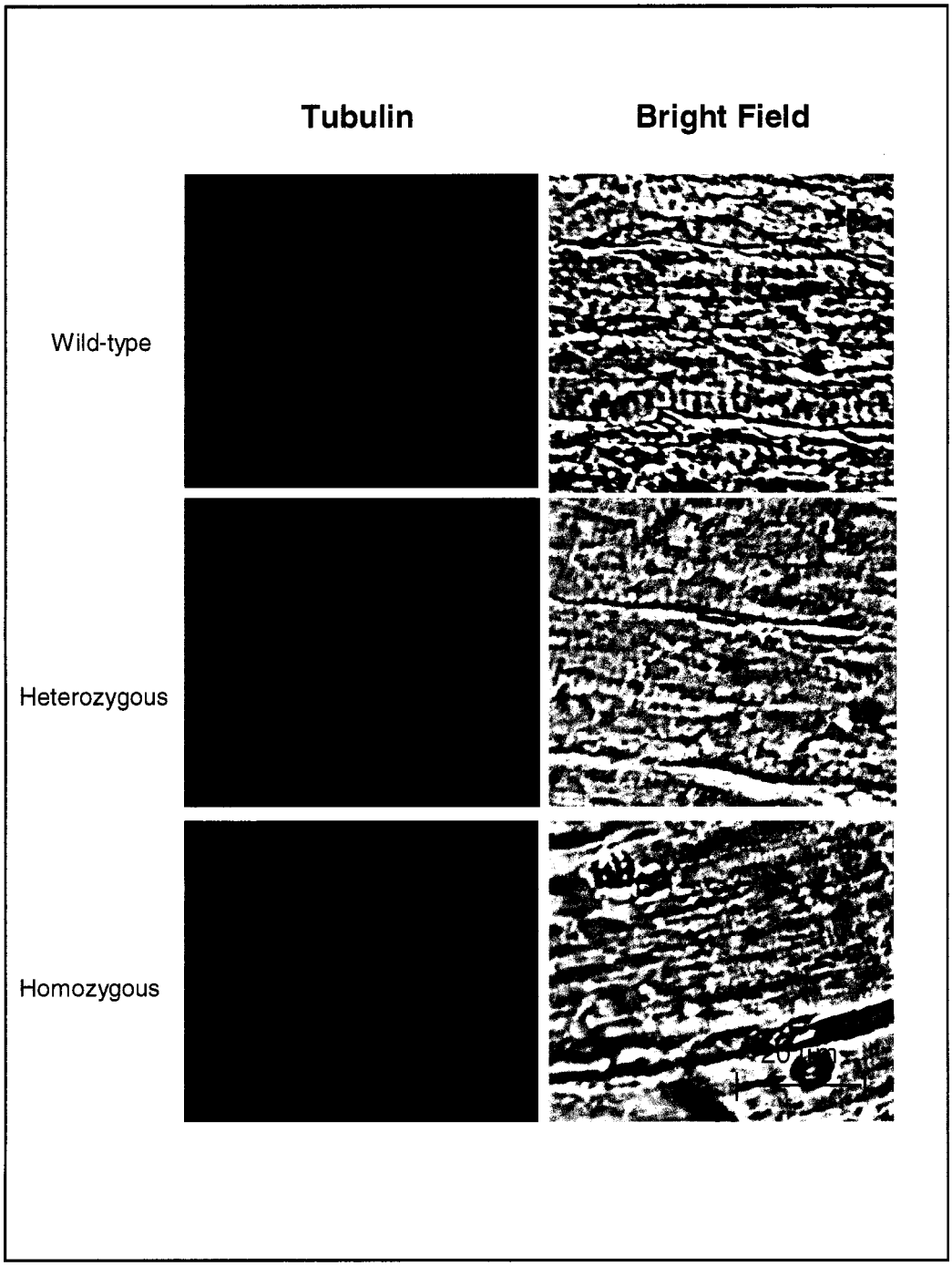

Figure 17 Fluorescence of the cytoskeletal protein α-tubulin (green) in longitudinal sections of tibialis anterior muscle from wild-type (A), heterozygous (C) and homozygous (E) mice. Nuclei are shown in blue (Hoechst). Tubulin immunoreactive product within sub-sarcolemmal and perinuclear regions (arrows A) is observed for wild-type and heterozygous mice (A, C). Approximately 52% of fibers from homozygous mice displayed reduced sub-sarcolemmal and perinuclear staining (arrow E).

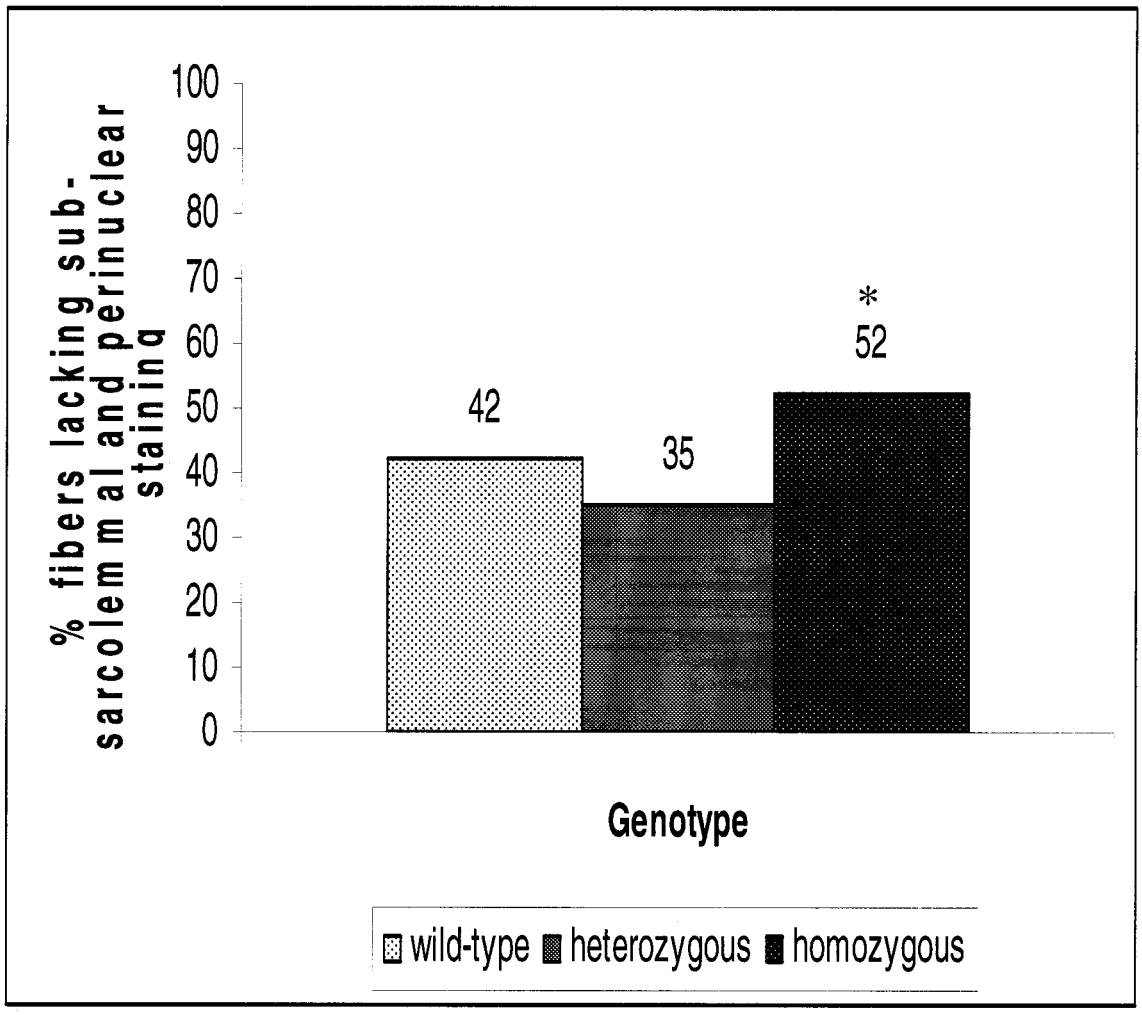

Figure 18 Loglinear analysis results. Observed frequency of muscle fibers displaying a lack of α–tubulin staining at the sub-sarcolemmal region. *Denotes significant differences from heterozygous values.

muscle fibers (Figure 19). Immunofluorescence experiments examining homozygous Bpag1-deficient muscle revealed an uneven cytoplasmic staining pattern with a dramatic loss of staining within the subsarcolemmal region of fibers. The staining pattern of over 230 muscle fibers was analyzed for wild-type (n=241), heterozygous (n=287) and homozygous (n=234) samples from a total of 4 mice for each genotype (Figure 20). Loglinear analysis was performed in order to assess and compare the observed frequency of muscle fibers displaying aberrant actin localization. The analyses reveal an increased frequency of homozygous muscle fibers (74%) displaying a loss of actin staining pattern, when compared to wild-type and heterozygous mice ($z>1.96$). Thus, the absence of Bpag1 has resulted in actin cytoskeletal disorganization in the form of uneven cytoplasmic staining patterns and a loss of sub-sarcolemmal staining as evidenced by immunofluorescence experiments. Results do not indicate a higher prevalence of disorganization among slow-twitch muscle fibers.

Additional assessments of the extent of actin co-localization with either desmin (Figure 21) or α-tubulin (Figure 22) was monitored by inspecting an overlap in staining (yellow), with Z-lines clearly defined, indicative of co-localization within this region. The extent of overlap was more apparent in wild-type and heterozygous muscle fibers, whereas the degree of overlap of the cytoskeletal elements was less apparent in homozygous muscle fibers as evidenced by distinct regions of staining. Thus, the lack of overlay staining patterns for actin with either desmin or tubulin would appear to indicate less co-localization of these elements in Bpag1-deficient muscle.

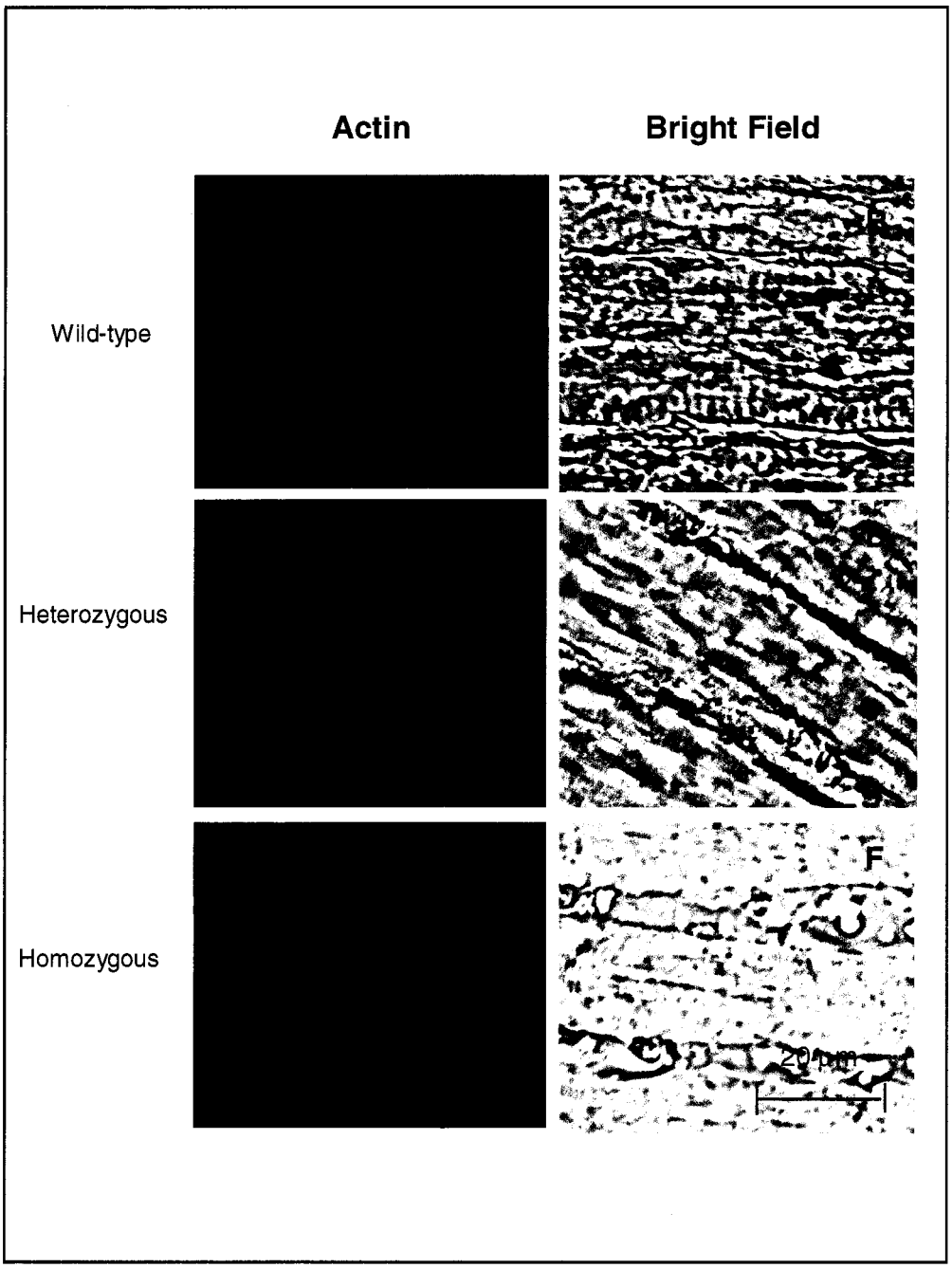

Figure 19 Fluorescence of the cytoskeletal protein actin (red) in longitudinal sections of tibialis anterior muscle from wild-type (A), heterozygous (C) and homozygous (E) mice. Nuclei are shown in blue (Hoechst). F-actin fluorescent product localized throughout the muscle fiber's cytoplasm, is observed for wild-type and heterozygous mice (A, C). Approximately 74% of fibers from homozygous mice displayed a loss of actin staining particularly within the sub-sarcolemmal region (arrow) as well as a patchy staining pattern.

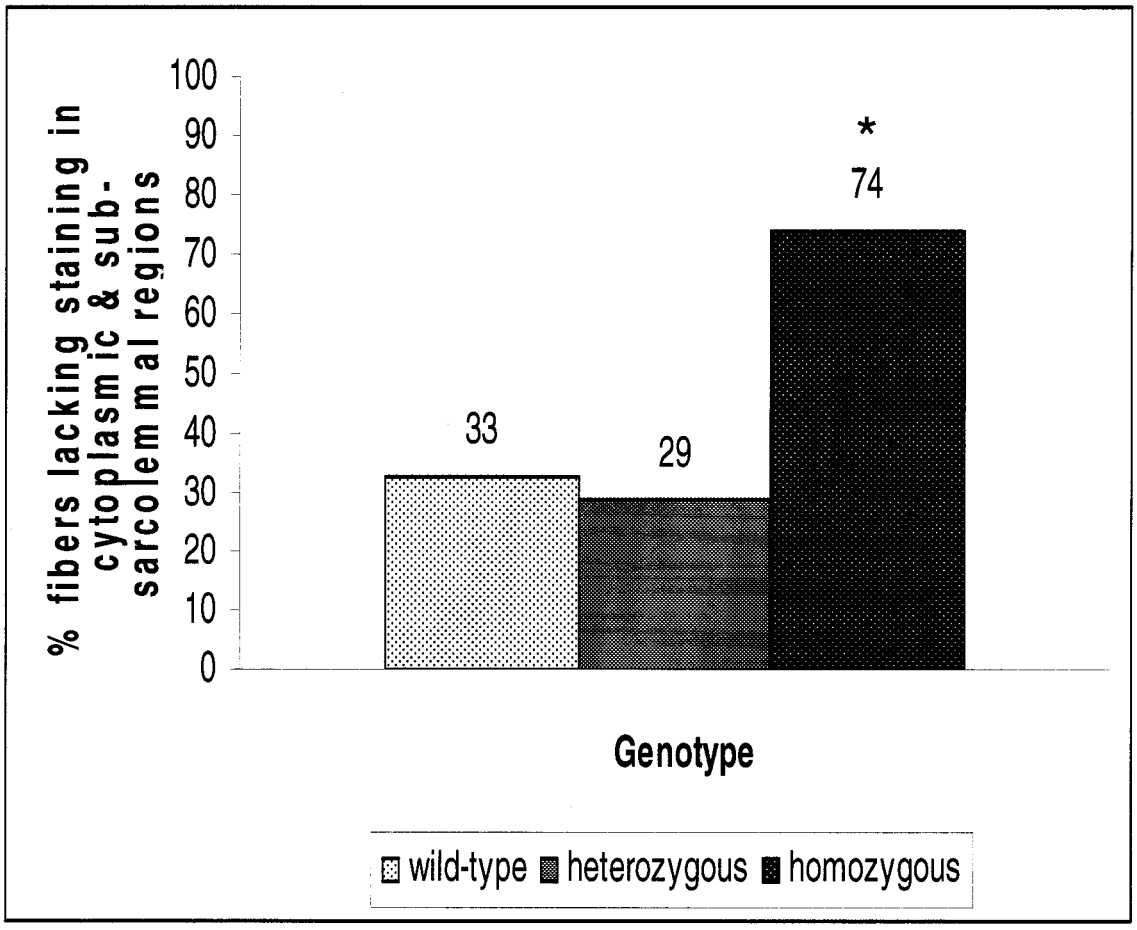

Figure 20 Loglinear analysis results. Observed frequency of muscle fibers displaying actin staining throughout the cytoplasmic and subsarcolemmal regions. *Denotes significant differences according to genotype (z>1.96).

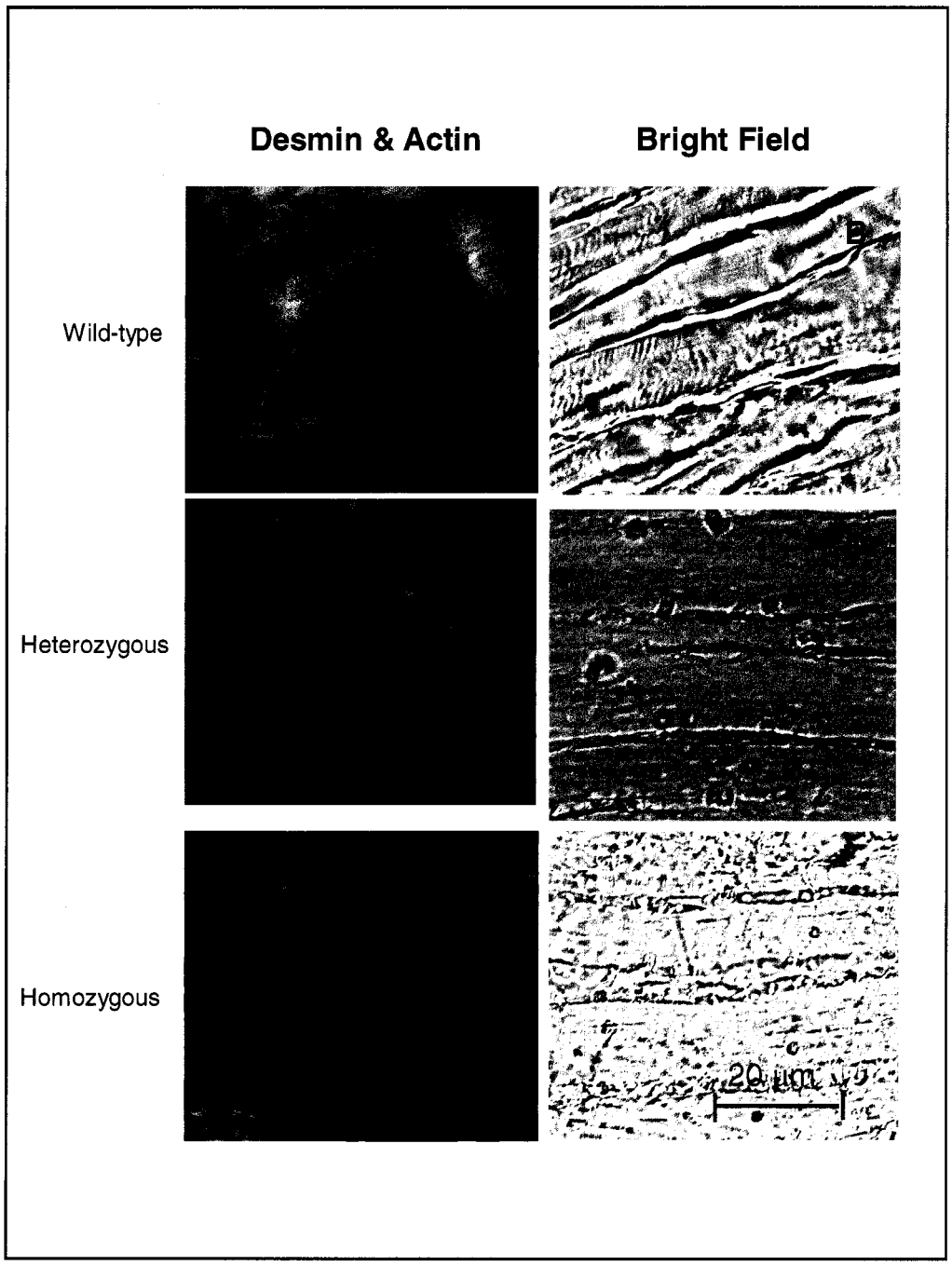

Figure 21 Fluorescence of the cytoskeletal proteins desmin(green) and α-actin (red), as well as nuclei (blue), in longitudinal sections of tibialis anterior muscle from wild-type (A), heterozygous (C) and homozygous (E) mice. Shown are overlayed images collected using FITC, Rhodamine and DAPI channels. Co-localization of desmin and actin is evident (arrow A) in wild-type and heterozygous muscle fibers (orange), but less clearly apparent in homozygous muscle fibers.

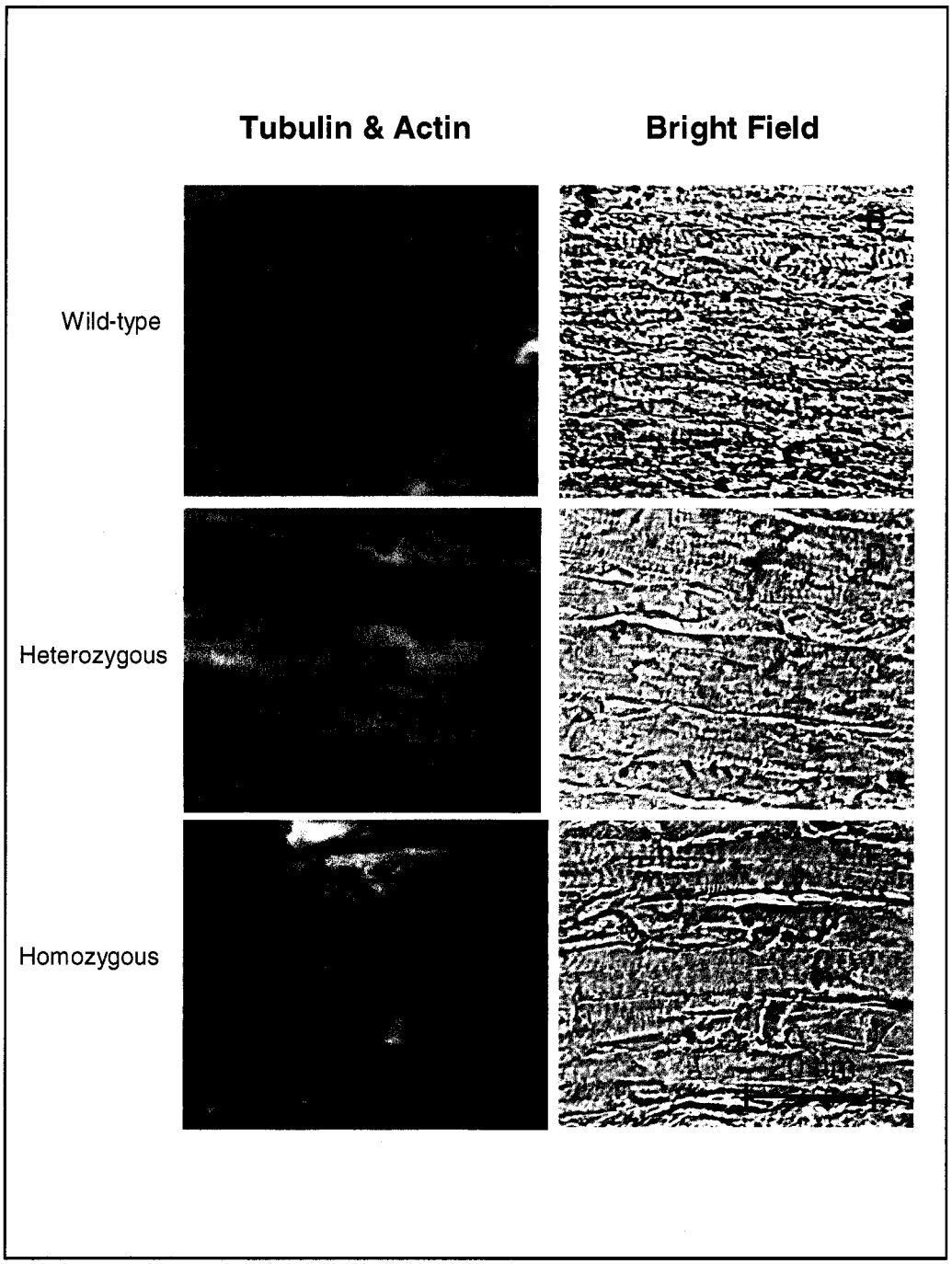

Figure 22 Fluorescence of the cytoskeletal proteins α-tubulin (green) and α-actin (red), as well as nuclei (blue), in longitudinal sections of tibialis anterior muscle from wild-type (A), heterozygous (C) and homozygous (E) mice. Shown are overlayed images collected using FITC, Rhodamine and DAPI channels. Co-localization of α-tubulin and α-actin (arrow A) is evident in wild-type and heterozygous muscle fibers (orange), but less clearly apparent in homozygous muscle fibers.

Discussion

Bpag1 is a gigantic crosslinking protein that harbors interaction domains for all three major components of the cytoskeleton. Mice that do not express Bpag1 molecules display a prominent limb incoordination phenotype as well as distinct neuronal, epithelial, skeletal muscle and Schwann cell aberrations. To investigate the role of Bpag1 in skeletal muscle in more detail, we assessed the expression levels and the cellular localization of muscle cytoskeletal proteins namely microfilaments, desmin intermediate filaments and microtubules in Bpag1-deficient (*dt*) hindlimb muscles. Our results indicate that the absence of Bpag1 expression in skeletal muscle leads to a significant reduction in the abundance of MF and MT subunits, and that all cytoskeletal components studied are differentially localized. Collectively, these data suggest that Bpag1 plays a role in regulating the cytoskeletal organization of these architectural elements in skeletal muscle.

The Expression Levels of Microfilament and Microtubule subunits are Reduced in Bpag1-deficient Skeletal Muscle

In the first set of experiments, we compared the protein levels of α-actin, α-tubulin and desmin in the hindlimb muscles of wild-type, heterozogous and homozygous *dt* mice. Our data revealed significant reductions in the amount of α-actin and α-tubulin protein levels in the hindlimb muscles of homozygous mice from the dt^{Tg4} line of transgenic animals whereas the levels of desmin protein were virtually unaffected.

Interestingly, reductions in the levels of α-tubulin subunits were observed specifically in soleus muscles which have a relatively high proportion of slow-twitch fibers (for example see (Girgenrath et al. 2005). These results indicate that the impact of Bpag1-deficiency appears to be specific to MFs and MTs and that, other mechanisms ensure normal levels of desmin subunits.

The molecular mechanisms underlying the reduction in the protein abundance of α-actin and of α-tubulin, and the maintenance of desmin protein levels, are likely linked to pre- or post-translational events or alternatively a combination of the two. Pre-translational events include changes in gene transcription and/or changes in mRNA stability. Indeed, the contribution of mRNA stability mechanisms have been reported for transcripts encoding skeletal muscle proteins such as mitochondrial enzymes, subsarcolemmal cytoskeletal proteins and neuromuscular junction components (Freyssenet et al. 1999; Boudreau-Lariviere et al. 2000; Jasmin et al. 2002). Measuring the abundance of transcripts encoding α-actin, α-tubulin and desmin in skeletal muscle from wild-type and homozygous mice, using standard molecular biology approaches, such as northern blots or RT-PCR, would serve to assess the involvement of pre-translational events.

Post-translational events include modifications in protein stability including longevity, or protein turnover. Determining the extent of protein turnover in skeletal muscle from wild-type versus homozygous mice using radio-labeled amino acids could help clarify the contribution of translational and post-translational events. Although

increased protein turnover is a possibility in skeletal muscle lacking Bpag1, it is worth noting that this process is likely to be specific to select proteins rather than a non-specific generalized response of all muscle proteins given that desmin protein levels were not found to be altered in homozygous *dt* muscle.

Microfilament Perturbations in Skeletal Muscle from *dt* Mice

In the present study, we have found that the levels of actin were significantly reduced and that the microfilament network was significantly altered in Bpag1-deficient skeletal muscle fibers. These results were not unexpected given that certain lines of evidence indicate that Bpag1 molecules are able to interact with the microfilament cytoskeleton of myogenic cells and are thought to stabilize the network (Dalpé et al., 1999; Young et al, 2003). Furthermore, a recent study has revealed that the interaction of Bpag1 molecules with the microfilament network in fact affects the actin filament dynamics. More specifically, it was demonstrated that the expression of a FLAG-tagged fusion protein harboring the Bpag1a/b2 unique region and the ABD had an impact on the bundling of microfilaments in C2C12 cells (Young et al., 2003). The loss of Bpag1 expression may therefore have a significant destabilization effect on actin filaments by altering their bundling capabilities. Indeed the involvement of plectin, another plakin crosslinker, in directing the actin dynamics in plectin-null fibroblasts and astroglial cell cultures was also previously reported (Andra et al., 1998). Surprisingly, in this latter study, plectin-deficiency was associated with a transient stabilization of the actin cytoskeleton. It may be argued that the stabilization effect of plakins on the

microfilament network may be cell specific and may vary between plakin family members. Taken together, these results would lend support to the notion that links between Bpag1 molecules and the actin-filament network not only contribute to the structural integrity of muscle cells but also regulate the stability of the microfilament network in skeletal muscle tissue.

Alterations in the Microtubule Network of Skeletal Muscle from *dt* Mice

The microtubule network of skeletal muscle fibers has received less attention compared to the microfilament and intermediate filament architecture and its function in contractile cells is only now emerging. Microtubules are typically located near myonuclei as well as within both sarcoplasmic and subsarcolemmal regions of muscle fibers (Park et al. 1984; Kano et al. 1991; Boudriau et al. 1993; Ralston et al. 1999). Results from the current study indicate that, in addition to reduced levels of α-tubulin building blocks, the microtubule lattice is significantly altered in the absence of Bpag1 expression as evidenced by reductions in subsarcolemmal staining and uneven sarcoplasmic staining. It is likely that disruption of the microtubule filament structure in *dt* skeletal muscle occurs post-natally given that perturbations of the microtubule system during myogenesis has been reported to have deleterious effects on both the fusion and differentiation potential of myogenic cells (Antin et al., 1981, Saitoh et al., 1988). This was in fact not observed in Bpag1-deficient primary myogenic cultures (Boudreau-Larivière and Kothary, 2002). Specifically, myoblast proliferation and differentiation were found to occur largely unaffected in these primary myogenic cells. Furthermore,

the skeletal muscle system of newborn Bpag1-deficient mice appears to be relatively normal compared to wild-type littermates (Dalpé et al., 1999). Taken together, it would appear that Bpag1 molecules may play a significant role in maintaining the microtubule lattice during post-natal skeletal muscle development whereas other microtubule-binding cytoskeletal elements such as MAP4 or MURF-3 (Mangan and Olmsted 1996, Spencer et al., 2000) may be more involved in establishing the microtubule system during myogenic pre-natal development.

Microtubules are essential in mitosis and their function in post-mitotic striated muscle cells is therefore intriguing. It has been suggested that the microtubule network plays an important role in localizing nuclei within the subsarcolemmal regions of skeletal muscle fibers (Boudriau et al., 1993). This characteristic placement of nuclei in skeletal muscle fibers in turn likely impacts nuclear transcriptional processes. The intimate link between microtubles and the organization of the Golgi complex and related structures in rodents has also been reported (Ralston et al., 1999). Indeed it will be interesting to see whether these organelles are in fact mislocalized or their organization perturbed in Bpag1-deficient skeletal muscle. This would have functional implications in that the Golgi complex is involved in glycosylation and the synthesis of transmembrane proteins and lipids.

Disorganization of the Desmin Intermediate Filament Network and Its Implications

Intermediate filaments, and in particular desmin, have been extensively studied and have been shown to be key components of the cytoskeletal architecture of contractile cells. In skeletal muscle fibers, desmin is localized at Z-lines and costameres and is thought to ensure proper myofibril alignment and to link peripheral myofibrils with the sarcolemma (reviewed in Clark et al., 2002). In the present investigation, we demonstrate that Bpag1-deficiency is associated with considerable alterations in the cellular localization of the desmin intermediate filament network. Specifically, immunofluorescence analysis of Bpag1-deficient muscles reveals loss of desmin Z-line staining and significant levels of desmin aggregation and clumping. Colocalization of desmin and Bpag1 molecules in C2C12 myogenic cells has been previously reported using indirect immunofluorescence analyses thereby suggesting a direct or indirect association between these two cytoskeletal molecules (Dalpé et al., 1999). Immunoelectron microscopy studies using Bpag1 and desmin antibodies would help further define the cellular linkage between these structural molecules.

The desmin cytoskeletal network has been implicated in regulating the cellular localization of organelles including mitochondria and perhaps nuclei. Indirect immunogold labeling of desmin in skeletal muscle has revealed a close association between mitochondria and this intermediate filament lattice in the vicinity of Z-discs (Reipert et al., 1999). Skeletal muscle from desmin-null mice have been shown to display increased mitochondrial clumping within the subsarcolemmal compartment of

muscle fibers and a reduction in the number of mitochondria between myofibrils thereby demonstrating the importance of desmin filaments in directing the cellular placement of mitochondria (Milner et al., 2000). Interestingly, ablation of the Bpag1 gene has been shown to result in a similar muscle fiber phenotype. More specifically, the occurrence of large mitochondrial aggregates under the muscle membrane was reported to be higher in Bpag1-deficient skeletal muscle compared to wild-type as revealed by ultrastructural analyses (Dalpé et al., 1999). Whether Bpag1 is directly or indirectly implicated in linking mitochondria to Z-lines in conjunction with desmin filaments remains to be shown. In this regard, it is worth highlighting that a desmin-mitochondria bridging function has in fact been reported for plectin in skeletal muscle fibers (Reipert et al., 1999) although mitochondrial clumping in skeletal muscle fibers from plectin-null mice has not been documented. It is therefore possible that both Bpag1 and plectin may both cooperate with desmin to anchor mitochondria at appropriate sites within the muscle fibers.

Mitochondrial respiratory function has been shown to be related to mitochondrial localization within skeletal muscle fibers. Given the high energy requirements of skeletal muscle, understanding the cellular mechanisms that are implicated in transporting and localizing this organelle is therefore highly relevant. The metabolic function of mitochondria tested *in situ* is downregulated in desmin-null slow-twitch muscle fibers (Milner et al, 2000). This aberrant mitochondrial respiratory activity was correlated with mitochondrial aggregation within subsarcolemmal regions as demonstrated histochemically by staining skeletal muscle sections for succinate dehydrogenase, a

mitochondrial marker (Milner et al., 2000). Interestingly, mitochondrial abnormalities have also been reported in skeletal muscle tissue obtained from a human patient suffering from epidermolysis bullosa simplex with muscular dystrophy which is a condition caused by mutations of the human plectin gene (Schroder et al., 2002). Mitochondrial dysfunction is also likely to occur in Bpag1-deficient skeletal muscle although experimental evidence to address this issue has not yet been documented.

The impact of Bpag1-deficiency on the expression levels and cellular localization of other intermediate filaments such as vimentin, nestin, synemin, paranemin, and cytokeratins known to be produced in contractile cells is also worth exploring given their close link with the desmin filament system that appears to be destabilized in muscles from homozygous *dt* mice. Bpag1b1/2 isoforms which are predominantly expressed in striated muscle tissue harbor a novel IFBD2. The binding properties of this site have yet to be characterized and it is tempting to speculate that these muscle isoforms may have the ability to associate with these other elements of the intermediate filament network.

Development of Post-Natal Myopathy in *dt* Mice

Dystonia musculorum mice develop a post-natal muscular dystrophy that is characterized by sarcomeric disruption, thick Z-lines and increased clumping of mitochondria within the subsarcolemmal region of muscle fibers as revealed by electron microscopy (Dalpé et al., 1999). In addition, Bpag1-deficient muscles fibers are generally weaker, more fatiguable and display increased sarcolemmal fragility in

response to contraction-induced mechanical stress (Dalpé et al., 1999). This muscle phenotype is in fact very similar to that reported for mouse desmin-null skeletal muscle (Milner et al., 1997, 2000) and some of these features have been reported for other forms of genetically-based myopathies that are linked to mutations of genes encoding other cytoskeletal proteins. For example, skeletal muscles from plectin-null mice display disorganized Z-lines and areas of sarcolemmal disruption (Andra et al., 1997). In the context of the present study, the impact of Bpag1 molecules, on both the structural framework and the contractile function of skeletal muscle fibers, appears to be multifaceted given that at least three major components, namely microfilaments, desmin intermediate filaments and microtubule networks, are disorganized in Bpag1-deficient muscle cells. Adding, to this complex framework, is the possibility that plakins have the potential to heterodimerize (Geerts et al., 1999). Given that Bpag1, MACF and plectin molecules are synthesized in skeletal muscle fibers, a variety of plakin combinations are therefore plausible though this has yet to be demonstrated. This would suggest that ablation of one of these plakin genes could weaken the crosslinking function of another.

Bpag1 Isoform Diversity and Its Importance in Contractile Cells

The precise subcellular localization of Bpag1 molecules has yet to be clearly established in skeletal muscle tissue. This work has been hampered by the lack of availability of antibodies able to produce staining in skeletal muscle tissue. This localization information will provide important clues to further define the role of Bpag1

molecules in contractile tissue and will help further define the isoform-specific functions of the various forms of Bpag1 molecules.

Despite this technical limitation, one recent study of cultured C2C12 myogenic cells has begun to explore the isoform diversity issue using antibodies that target particular Bpag1 isoforms (Young et al., 2003). Antibodies specifically recognizing the unique N-terminal region of Bpag1a/b2 isoforms (muscle and neural) were found to decorate actin stress fibers throughout the cytoplasm and were also found to stain perinuclear as well as nuclear regions. The presence of a functional nuclear localization signal was identified within the plakin region which is likely responsible for the observed Bpag1a/b2 nuclear staining. Interestingly, a fusion protein containing the shorter unique N-terminal region of Bpag1a/b1 along with the plakin domain harboring the NLS was reported to localize almost exclusively to actin filaments and was excluded from the nuclei of transfected C2C12 cells. Isoform-specific subcellular localization has also been reported for plectin molecules in keratinocytes (Andra et al., 2003). Isoform diversity especially within the N-terminal region, is a feature of several plakin family members and its important function in targeting these molecules to specific locations in cells is being revealed. This may in turn contribute to the ability of these various isoforms to perform site-specific functions within cells.

Cytoskeletal proteins belonging to the spectrin superfamily, which includes Bpag1, have been shown to be expressed in the nuclei of a variety of cell types including myogenic cells (Young et al., 2003, for review see Young and Kothary, 2005). The

putative nuclear functions ascribed to these spectrin-related proteins include scaffolding for DNA-repair molecules and nuclear positioning (Young and Kothary, 2005). Furthermore, it has been suggested that specific isoforms of Bpag1 targeted to the nuclei may contribute to its architectural structure (Young and Kothary, 2005). Lamins, which are nuclear intermediate filaments, have been shown to contribute to the function and architectural organization of striated muscle cells and are thought to stabilize the nuclear envelope (reviewed in Clark et al., 2002 and Young and Kothary, 2005). A myopathy characterized by muscle weakness has been reported for lamin-A-null mice which underscores the important link between the contractile function of muscle and the organization and stability of myonuclei (Sullivan et al. 1991; Lenz-Bohme et al. 1997). Accordingly, it would be realistic to consider the involvement of Bpag1 molecules in organizing the lamin network of the inner nuclear membrane. In the context of the present study, it is therefore likely that the impact of ablating expression of the Bpag1 gene in skeletal muscle fibers may be more widespread than was previously thought. The structural abnormalities reported and hypothesized in other tissue types, such as cardiac muscle, may lead to further insight related to the functional aberrations reported by others. Indeed, it is plausible that both the cellular and nuclear architectural organization may be hindered in Bpag1-deficient muscle given that expression of all Bpag1 isoforms is inhibited in *dt* mice.

Cytoskeletal Perturbations Are Slightly More Pronounced in Highly Used Slow-twitch Muscles.

Fiber type-dependent differences in the cytoskeleton have been previously highlighted. For example, immunoblotting experiments by Boudriau et al. (1993) have demonstrated higher concentrations of α-tubulin in slow-twitch muscle fibers when compared to fast-twitch fibers. A higher abundance for desmin IF and dystrophin in slow-twitch fibers have also been reported (Ho-Kim and Rogers 1992; Chopard et al. 2001). While no significant differences were observed in the spatial orientation and organization of MTs between slow- and fast-twitch fibers, Boudriau et al. (1993) noted that the density of MTs within the sarcoplasmic and subsarcolemmal space was greater in slow- versus fast-twitch fibers (also reported by Ralston et al., 1999). It is possible that the higher content of various cytoskeletal proteins in highly recruited slow-twitch fibers likely underscores the need for enhanced structural stability in muscles that undergo lengthier periods of mechanical stress. Thus, we examined whether cytoskeletal disturbances observed in Bpag1-deficient muscle are more pronounced in highly used slow-twitch muscle. Of the three cytoskeletal filament subunits studied (α-actin, α-tubulin and desmin), two were downregulated in slow-twitch fibers (α-actin, α-tubulin) whereas only one was reduced in fast-twitch fibers (α-actin). In comparison, cytoskeletal perturbations observed by immunofluorescence were equally pronounced in both slow- and fast-twitch muscle fibers. The impact of Bpag1-deficiency is therefore slightly more pronounced in highly used muscle though not dramatically.

Skeletal Muscles from Wild-type and Heterozygous Mice Display a Similar Profile

The involvement of Bpag1 molecules in the process of peripheral nerve myelination has been previously reported (Bernier et al., 1998). Interestingly, in this

particular study, myelination abnormalities of peripheral nerves were reported not only for homozygous mice belonging to the dt^{Tg4} and dt^{27J} lines but also for heterozygous animals. A Bpag1 "dose effect" was therefore noted as it pertains to Schwann cell-mediated myelination. Although heterozygous animals do not display sensory neurodegeneration or the characteristic limb incoordination observed in homozygous mice, these animals did show a myelination phenotype that was intermediate to that displayed by wild-type and homozygous animals (Bernier et al., 1998). Until now, it was not known whether this "semi-dominant" profile also occurred in skeletal muscle. Based on our results, it appears that skeletal muscle from wild-type and heterozygous animals display similar cytoskeletal features, indicating that Bpag1 expression from one intact copy of the Bpag1 gene is sufficient to maintain levels of α-actin, desmin and α-tubulin protein expression and to preserve the cytoskeletal architecture noted in skeletal muscles from wild-type mice.

Limitations of the present study are primarily related to the statistical variability in accordance with the small sample size. More animals would be needed in order to obtain results that are more robust related to the impact of Bpag1-deficiency on the levels of desmin, α-tubulin and α-actin.

Conclusions

In the present study, the impact of Bpag1-deficiency on the expression levels of MF, IF and MT subunits, and the sub cellular localization of these cytoskeletal elements was assessed in skeletal muscle. Based on our results, we report that all three cytoskeletal networks studied, namely MFs, desmin IFs, and MTs are dependent on Bpag1 for their proper cytoskeletal localization. In addition, Bpag1-deficiency also coincides with reduced protein expression levels for α-actin and for α-tubulin. The data also indicate that highly used slow-twitch fibers are slightly more affected by ablating Bpag1 gene expression compared to fast-twitch fibers.

Finally, our findings indicate that the transcriptional activity of one intact Bpag1 allele, is sufficient to ensure the integrity of the MF, desmin IF and MT networks. As a whole, the present study has highlighted the important contribution of Bpag1 molecules in maintaining the structural integrity of the architectural framework of skeletal muscle fibers. What this investigation has also emphasized is the complex interactions and cooperativity taking place between the various cytoskeletal networks located in specific compartments of the skeletal muscle cells. Collectively, these many elements contribute to the functional and structural properties of contractile cells.

Further studies are needed in order to determine the specific mechanisms involving Bpag1 in directing the cellular localization of cytoskeletal proteins. At present, little is known about the role of Bpag1 in other tissue types, such as cardiac muscle, thus additional studies in such areas would therefore be beneficial.

REFERENCES

al-Ali, S. Y. and A. G. al-Zuhair (1989). "Fine structural study of the spinal cord and spinal ganglia in mice afflicted with a hereditary sensory neuropathy, dystonia musculorum." J Submicrosc Cytol Pathol **21**(4): 737-48.

Andra, K., H. Lassmann, et al. (1997). "Targeted inactivation of plectin reveals essential function in maintaining the integrity of skin, muscle, and heart cytoarchitecture." Genes Dev. **11**(23): 3143-56.

Andra, K., B. Nikolic, et al. (1998). "Not just scaffolding: plectin regulates actin dynamics in cultured cells." Genes Dev. **12**(21): 3442-51.

Andra, K., I. Kornacker, et al. (2003). "Plectin-isoform-specific rescue of hemidesmosomal defects in plectin (-/-) keratinocytes." J Invest Dermtol **120**(2): 189-97.

Antin, P. B., S. Forry-Schaudies, et al. (1981). "Taxol induces postmitotic myoblasts to assemble interdigitating microtubule-myosin arrays that exclude actin filaments." J Cell Biol **90**(2): 300-8.

Balogh, J., M. Merisckay, et al. (2002). "Hearts from mice lacking desmin have a myopathy with impaired active force generation and unaltered wall compliance." Cardiovasc Res **53**(2): 439-50.

Bernier, G., A. Brown, et al. (1995). "Dystonin transcripts are altered and their levels are reduced in the mouse neurological mutant dt24J." Biochem Cell Biol **73**(9-10): 605-9.

Bernier, G., Y. De Repentigny, et al. (1998). "Dystonin is an essential component of the Schwann cell cytoskeleton at the time of myelination." Development **125**(11): 2135-48.

Bernier, G. and R. Kothary (1998). "Prenatal onset of axonopathy in Dystonia musculorum mice." Dev Genet **22**(2): 160-8.

Berthier, C. and S. Blaineau (1997). "Supramolecular organization of the subsarcolemmal cytoskeleton of adult skeletal muscle fibers. A review." Biol Cell **89**(7): 413-34.

Bilak, S. R., S. W. Sernett, et al. (1998). "Properties of the novel intermediate filament protein synemin and its identification in mammalian muscle." Arch Biochem Biophys **355**(1): 63-76.

Boudreau-Lariviere, C., R. Y. Chan, et al. (2000). "Molecular mechanisms underlying the activity-linked alterations in acetylcholinesterase mRNAs in developing versus adult rat skeletal muscles." J Neurochem **74**(6): 2250-8.

Boudreau-Lariviere, C. and R. Kothary (2002). "Differentiation potential of primary myogenic cells derived from skeletal muscle of dystonia musculorum mice." Differentiation **70**(6): 247-56.

Boudriau, S., M. Vincent, et al. (1993). "Cytoskeletal structure of skeletal muscle: identification of an intricate exosarcomeric microtubule lattice in slow- and fast-twitch muscle fibers." J Histochem Cytochem **41**(7): 1013-21.

Brown, A., G. Bernier, et al. (1995). "The mouse dystonia musculorum gene is a neural isoform of bullous pemphigoid antigen 1." Nat Genet **10**(3): 301-6.

Campbell, R. M. and A. C. Peterson (1992). "An intrinsic neuronal defect operates in dystonia musculorum: a study of dt/dt<==>+/+ chimeras." Neuron **9**(4): 693-703.

Chopard, A., F. Pons, et al. (2001). "Cytoskeletal protein contents before and after hindlimb suspension in a fast and slow rat skeletal muscle." Am J Physiol Regul Integr Comp Physiol **280**(2): R323-30.

Clark, K. A., A. S. McElhinny, et al. (2002). "Striated muscle cytoarchitecture: an intricate web of form and function." Annu Rev Cell Dev Biol **18**: 637-706.

Dalpe, G., N. Leclerc, et al. (1998). "Dystonin is essential for maintaining neuronal cytoskeleton organization." Mol Cell Neurosci **10**(5-6): 243-57.

Dalpe, G., M. Mathieu, et al. (1999). "Dystonin-deficient mice exhibit an intrinsic muscle weakness and an instability of skeletal muscle cytoarchitecture." Dev Biol **210**(2): 367-80.

De Repentigny, Y., J. Deschenes-Furry, et al. (2003). "Impaired fast axonal transport in neurons of the sciatic nerves from dystonia musculorum mice." J Neurochem **86**(3): 564-71.

Dowling, J., Y. Yang, et al. (1997). "Developmental expression of BPAG1-n: insights into the spastic ataxia and gross neurologic degeneration in dystonia musculorum mice." Dev Biol **187**(2): 131-42.

Duchen, L. W. (1976). "Dystonia musculorum--an inherited disease of the nervous system in the mouse." Adv Neurol **14**: 353-65.

Duchen, L. W., S. J. Strich, et al. (1964). "Clinical and Pathological Studies of an Hereditary Neuropathy in Mice (Dystonia Musculorum)." Brain **87**: 367-78.

Ellisman, M. H. and K. R. Porter (1980). "Microtrabecular structure of the axoplasmic matrix: visualization of cross-linking structures and their distribution." J Cell Biol **87**(2 Pt 1): 464-79.

Foisner, R., W. Bohn, et al. (1995). "Distribution and ultrastructure of plectin arrays in subclones of rat glioma C6 cells differing in intermediate filament protein (vimentin) expression." J Struct Biol **115**(3): 304-17.

Franke, W. W., E. Schmid, et al. (1978). "The intermediate-sized filaments in rat kangaroo PtK2 cells. II. Structure and composition of isolated filaments." Cytobiologie **17**(2): 392-411.

Freyssenet, D., M. K. Connor, et al. (1999). "Cytochrome c transcriptional activation and mRNA stability during contractile activity in skeletal muscle." Am J Physiol **277**(1 Pt 1): E26-32.

Fuchs, E. and K. Weber (1994). "Intermediate filaments: structure, dynamics, function, and disease." Annu Rev Biochem **63**: 345-82.

Geerts, D., L. Fontao, et al. (1999). "Binding of integrin alpha6beta4 to plectin prevents plectin association with F-actin but does not interfere with intermediate filament binding." J Cell Biol **147**(2): 417-34.

German, W. J. and Stanfield, C. L. (2002). "Principles of Human Physiology." Pearson Education Inc 813 pages.

Girgenrath, S., K. Song, et al. (2005). "Loss of myostatin expression alters fiber-type distribution and expression of myosin heavy chain isoforms in slow- and fast-type skeletal muscle." Muscle Nerve **31**(1): 34-40.

Granger, B. L. and E. Lazarides (1978). "The existence of an insoluble Z disc scaffold in chicken skeletal muscle." Cell **15**(4): 1253-68.

Granger, B. L. and E. Lazarides (1979). "Desmin and vimentin coexist at the periphery of the myofibril Z disc." Cell **18**(4): 1053-63.

Guo, L., L. Degenstein, et al. (1995). "Gene targeting of BPAG1: abnormalities in mechanical strength and cell migration in stratified epithelia and neurologic degeneration." Cell **81**(2): 233-43.

Heggeness, M. H., M. Simon, et al. (1978). "Association of mitochondria with microtubules in cultured cells." Proc Natl Acad Sci U S A **75**(8): 3863-6.

Hirokawa, N. (1982). "Cross-linker system between neurofilaments, microtubules, and membranous organelles in frog axons revealed by the quick-freeze, deep-etching method." J Cell Biol **94**(1): 129-42.

Ho-Kim, M. A. and P. A. Rogers (1992). "Quantitative analysis of dystrophin in fast- and slow-twitch mammalian skeletal muscle." FEBS Lett **304**(2-3): 187-91.

Ilkovski, B., S. T. Cooper, et al. (2001). "Nemaline myopathy caused by mutations in the muscle alpha-skeletal-actin gene." Am J Hum Genet **68**(6): 1333-43.

Janota, I. (1972). "Ultrastructural studies of an hereditary sensory neuropathy in mice (dystonia musculorum)." Brain **95**(3): 529-36.

Jasmin, B. J., L. M. Angus, et al. (2002). "Multiple regulatory events controlling the expression and localization of utrophin in skeletal muscle fibers: insights into a therapeutic strategy for Duchenne muscular dystrophy." J Physiol Paris **96**(1-2): 31-42.

Jefferson, J. J., C. L. Leung, et al. (2004). "Plakins: goliaths that link cell junctions and the cytoskeleton." Nat Rev Mol Cell Biol **5**(7): 542-53.

Jones, J. C., J. Asmuth, et al. (1994). "Hemidesmosomes: extracellular matrix/intermediate filament connectors." Exp Cell Res **213**(1): 1-11.

Kano, Y., N. Fujimaki, et al. (1991). "The distribution and arrangement of microtubules in mammalian skeletal muscle fibers." Cell Struct Funct **16**(3): 251-61.

Kaufmann, U., J. Kirsch, et al. (1999). "The M-cadherin catenin complex interacts with microtubules in skeletal muscle cells: implications for the fusion of myoblasts." J Cell Sci **112 (Pt 1)**: 55-68.

Khaitlina, S. Y. (2001). "Functional specificity of actin isoforms." Int Rev Cytol **202**: 35-98.

Kosmehl, H., L. Langbein, et al. (1990). "Transient cytokeratin expression in skeletal muscle during murine embryogenesis." Anat Anz **171**(1): 39-44.

Kothary, R., S. Clapoff, et al. (1988). "A transgene containing lacZ inserted into the dystonia locus is expressed in neural tube." Nature **335**(6189): 435-7.

Lazarides, E. (1980a). "Desmin and intermediate filaments in muscle cells." Results Probl Cell Differ **11**: 124-31.

Lazarides, E. (1980b). "Intermediate filaments as mechanical integrators of cellular space." Nature **283**(5744): 249-256.

Lenz-Bohme, B., J. Wismar, et al. (1997). "Insertional mutation of the Drosophila nuclear lamin Dm0 gene results in defective nuclear envelopes, clustering of nuclear pore complexes, and accumulation of annulate lamellae." J Cell Biol **137**(5): 1001-16.

Leung, C. L., K. J. Green, et al. (2002). "Plakins: a family of versatile cytolinker proteins." Trends Cell Biol **12**(1): 37-45.

Leung, C. L., R. K. Liem, et al. (2001a). "The plakin family." J Cell Sci **114**(Pt 19): 3409-10.

Leung, C. L., D. Sun, et al. (1999). "The intermediate filament protein peripherin is the specific interaction partner of mouse BPAG1-n (dystonin) in neurons." J Cell Biol **144**(3): 435-46.

Leung, C. L., M. Zheng, et al. (2001b). "The BPAG1 locus: Alternative splicing produces multiple isoforms with distinct cytoskeletal linker domains, including predominant isoforms in neurons and muscles." J Cell Biol **154**(4): 691-7.

Li, Z., M. Mericskay, et al. (1997). "Desmin is essential for the tensile strength and integrity of myofibrils but not for myogenic commitment, differentiation, and fusion of skeletal muscle." J Cell Biol **139**(1): 129-44.

Mangan, M. E. and J. B. Olmsted (1996). "The gene for microtubule-associated protein 4 (Mtap4) maps to the distal region of mouse chromosome 9." Mamm Genome **7**(12): 918-9.

Markwald, R. R. (1973). "Distribution and relationship of precursor Z material to organizing myofibrillar bundles in embryonic rat and hamster ventricular myocytes." J Mol Cell Cardiol **5**(4): 341-50.

Messer, A. and N. L. Strominger (1980). "An allele of the mouse mutant dystonia musculorum exhibits lesions in red nucleus and striatum." Neuroscience **5**(3): 543-9.

Milner, D. J., M. Mavroidis, et al. (2000). "Desmin cytoskeleton linked to muscle mitochondrial distribution and respiratory function." J Cell Biol **150**(6): 1283-98.

Milner, D. J., G. E. Taffet, et al. (1999). "The absence of desmin leads to cardiomyocyte hypertrophy and cardiac dilation with compromised systolic function." J Mol Cell Cardiol **31**(11): 2063-76.

Milner, D.J., Y. Capetanaki, & G. Weitzer (1997). "Desmin in muscle formation and maintenance: knockouts and consequences." Cell Struct Funct **22**(1): 103-16.

Milner, D. J., G. Weitzer, et al. (1996). "Disruption of muscle architecture and myocardial degeneration in mice lacking desmin." J Cell Biol **134**(5): 1255-70.

Minoshima, S., M. Amagai, et al. (1991). "Localization of the human gene for 230-kDal bullous pemphigoid autoantigen (BPAG1) to chromosome 6pter----q15." Cytogenet Cell Genet **57**(1): 30-2.

Mizuno, Y., T. G. Thompson, et al. (2001). "Desmuslin, an intermediate filament protein that interacts with alpha -dystrobrevin and desmin." Proc Natl Acad Sci U S A **98**(11): 6156-61.

Mueller, S., V. Klaus-Kovtun, et al. (1989). "A 230-kD basic protein is the major bullous pemphigoid antigen." J Invest Dermatol **92**(1): 33-8.

Newey, S. E., E. V. Howman, et al. (2001). "Syncoilin, a novel member of the intermediate filament superfamily that interacts with alpha-dystrobrevin in skeletal muscle." J Biol Chem **276**(9): 6645-55.

Nowak, K. J., D. Wattanasirichaigoon, et al. (1999). "Mutations in the skeletal muscle alpha-actin gene in patients with actin myopathy and nemaline myopathy." Nat Genet **23**(2): 208-12.

Park, R. S., M. F. Legier, et al. (1984). "Perinuclear microtubules in postnatal rat heart." J Morphol **179**(1): 13-9.

Pascual, J., M. Pfuhl, et al. (1997). "Solution structure of the spectrin repeat: a left-handed antiparallel triple-helical coiled-coil." J Mol Biol **273**(3): 740-51.

Pette, D. and R. S. Staron (2001). "Transitions of muscle fiber phenotypic profiles." Histochem Cell Biol **115**(5): 359-72.

Poon, E., E. V. Howman, et al. (2002). "Association of syncoilin and desmin: linking intermediate filament proteins to the dystrophin-associated protein complex." J Biol Chem **277**(5): 3433-9.

Portier, M. M., B. de Nechaud, et al. (1983). "Peripherin, a new member of the intermediate filament protein family." Dev Neurosci **6**(6): 335-44.

Price, M. G. and E. Lazarides (1983). "Expression of intermediate filament-associated proteins paranemin and synemin in chicken development." J Cell Biol **97**(6): 1860-74.

Ralston, E., T. Ploug, et al. (2001) "Golgi complex, endoplasmic reticulum exit sites, and microtubules in skeletal muscle fibers are organized by patterned activity." J Neurosci **21**(3): 875-83.

Ralston, E., Z. Lu, et al. (1999). "The organization of the Golgi complex and microtubules in skeletal muscle is fiber type-dependent." J Neurosci **19**(24): 10694-705.

Reipert, S., F. Steinbock, et al. (1999). "Association of mitochondrial with plectin and desmin intermediate filaments in striated muscle." Exp Cell Res. **252**(2): 479-91.

Rezniczek, G. A., J. M. de Pereda, et al. (1998). "Linking integrin alpha6beta4-based cell adhesion to the intermediate filament cytoskeleton: direct interaction between the beta4 subunit and plectin at multiple molecular sites." J Cell Biol **141**(1): 209-25.

Roper, K., S. L. Gregory, et al. (2002). "The 'spectraplakins': cytoskeletal giants with characteristics of both spectrin and plakin families." J Cell Sci **115**(Pt 22): 4215-25.

Rubenstein, P. A. and J. A. Spudich (1977). "Actin microheterogeneity in chick embryo fibroblasts." Proc Natl Acad Sci U S A **74**(1): 120-3.

Ruhrberg, C. and F. M. Watt (1997). "The plakin family: versatile organizers of cytoskeletal architecture." Curr Opin Genet Dev **7**(3): 392-7.

Saitoh, O., T. Arai, et al. (1988). "Distribution of microtubules and other cytoskeletal filaments during myotube elongation as revealed by fluorescence microscopy." Cell Tissue Res **252**(2): 263-73.

Schroder, R., W.S. Kunz, et al. (2002). "Disorganization of the desmin cytoskeleton and mitochondrial dysfunction in plectin-related epidermolysis bullosa symplex with muscular dystrophy." J Neuropathol Exp Neuro **61**(6): 520-30.

Schultz, J., F. Milpetz, et al. (1998). "SMART, a simple modular architecture research tool: identification of signaling domains." Proc Natl Acad Sci U S A **95**(11): 5857-64.

Sejersen, T. and U. Lendahl (1993). "Transient expression of the intermediate filament nestin during skeletal muscle development." J Cell Sci **106 (Pt 4)**: 1291-300.

Shah, S. B., F. C. Su, et al. (2002). "Evidence for increased myofibrillar mobility in desmin-null mouse skeletal muscle." J Exp Biol **205**(Pt 3): 321-5.

Sheterline, P., J. Clayton, et al. (1995). "Actin." Protein Profile **2**(1): 1-103.

Sjoberg, G., L. Edstrom, et al. (1994). "Myofibers from Duchenne/Becker muscular dystrophy and myositis express the intermediate filament nestin." J Neuropathol Exp Neurol **53**(4): 416-23.

Sotelo, C. and J. L. Guenet (1988). "Pathologic changes in the CNS of dystonia musculorum mutant mouse: an animal model for human spinocerebellar ataxia." Neuroscience **27**(2): 403-24.

Spencer, J. A., S. Eliazer, et al. (2000). "Regulation of microtubule dynamics and myogenic differentiation by MURF, a striated muscle RING-finger protein." J Cell Biol **150**(4): 771-84.

Stanley, J. R. (1993). "Cell adhesion molecules as targets of autoantibodies in pemphigus and pemphigoid, bullous diseases due to defective epidermal cell adhesion." Adv Immunol **53**: 291-325.

Stephens, R. E. and K. T. Edds (1976). "Microtubules: structure, chemistry, and function." Physiol Rev **56**(4): 709-77.

Storti, R. V., D. M. Coen, et al. (1976). "Tissue-specific forms of actin in the developing chick." Cell **8**(4): 521-7.

Sullivan, A. T., D. J. Baker, et al. (1991). "Effect of calcium channel blocking agents on infarct size after ischaemia-reperfusion in anaesthetised pigs: relationship between cardioprotection and cardiodepression." J Cardiovasc Pharmacol **17**(5): 707-17.

Sun, D., C. L. Leung, et al. (2001). "Characterization of the microtubule binding domain of microtubule actin crosslinking factor (MACF): identification of a novel group of microtubule associated proteins." J Cell Sci **114**(Pt 1): 161-172.

Tokuyasu, K. T., A. H. Dutton, et al. (1983a). "Immunoelectron microscopic studies of desmin (skeletin) localization and intermediate filament organization in chicken cardiac muscle." J Cell Biol **96**(6): 1736-42.

Tokuyasu, K. T., A. H. Dutton, et al. (1983b). "Immunoelectron microscopic studies of desmin (skeletin) localization and intermediate filament organization in chicken skeletal muscle." J Cell Biol **96**(6): 1727-35.

Vandekerckhove, J. and K. Weber (1979). "The complete amino acid sequence of actins from bovine aorta, bovine heart, bovine fast skeletal muscle, and rabbit slow skeletal muscle. A protein-chemical analysis of muscle actin differentiation." Differentiation **14**(3): 123-33.

Yang, Y., C. Bauer, et al. (1999). "Integrators of the cytoskeleton that stabilize microtubules." Cell **98**(2): 229-38.

Yang, Y., J. Dowling, et al. (1996). "An essential cytoskeletal linker protein connecting actin microfilaments to intermediate filaments." Cell **86**(4): 655-65.

Young, K. G., M. Pool, et al. (2003). "Bpag1 localization to actin filaments and to the nucleus is regulated by its N-terminus." J Cell Sci **116**(Pt 22): 4543-55.

Young, K. G. and Kothary, R. (2005). "Spectrin repeat proteins in the nucleus." Bioessays **27**(2): 144-52.

Zimmerman, L., B. Parr, et al. (1994). "Independent regulatory elements in the nestin gene direct transgene expression to neural stem cells or muscle precursors." Neuron **12**(1): 11-24.

APPENDICES

Appendix A: Mouse Information

Mouse ID * Genotype

Western Blot	*Mouse ID*	*Genotype*
Set #1		
	B6-14	Wt
	B6-16	Ht
	B6-21	*dt*
Set #2		
	A2-24	Wt
	A2-25	Ht
	A2-20	*dt*
Set #3		
	B5-11	Wt
	B5-12	Ht
	B5-17	*dt*
Set #4		
	B5-16	Wt
	B5-15	Ht
	B5-18	*dt*
Immunofluorescence		
Set #1		
	B5-23	Wt
	B5-19	Ht
	B5-24	*dt*
Set #2		
	B4-31	Wt
	B4-30	Ht
	B4-24	*dt*
Set #3		
	B6-26	Wt
	B6-28	Ht
	B6-30	*dt*
Set #4		
	B6-29	Wt
	B6-27	Ht
	B6-31	*dt*

Appendix B: Raw Data

Western blot analysis.

Genotype	Protein	Muscle Type	Densitometric Values	Percentage
Set #1				
Homozygous	Desmin	Slow-twitch	15.93	112
Wild-type	Desmin	Slow-twitch	14.19	100
Heterozygous	Desmin	Slow-twitch	9.94	70
Wild-gype	Desmin	Slow-twitch	13.18	100
Heterozygous	Desmin	Slow-twitch	5.76	44
homozygous	Desmin	Slow-twitch	12.59	95
Set #2				
Wild-type	Desmin	Slow-twitch	9.25	100
Heterozygous	Desmin	Slow-twitch	6.79	73
Homozygous	Desmin	Slow-twitch	8.71	94
Wild-type	Desmin	Slow-twitch	7.47	100
Heterozygous	Desmin	Slow-twitch	8.99	120
Homozygous	Desmin	Slow-twitch	7.85	105
Set #1				
Wild-type	Tubulin	Slow-twitch	4.01	100
Heterozygous	Tubulin	Slow-twitch	1.86	46
Homozygous	Tubulin	Slow-twitch	1.29	32
Wild-type	Tubulin	Slow-twitch	2.03	100
Heterozygous	Tubulin	Slow-twitch	1.79	88
Homozygous	Tubulin	Slow-twitch	1.36	67
Set #2				
Wild-type	Tubulin	Slow-twitch	32.20	100
Heterozygous	Tubulin	Slow-twitch	29.61	92
Homozygous	Tubulin	Slow-twitch	12.95	40
Wild-type	Tubulin	Slow-twitch	10.11	100
Heterozygous	Tubulin	Slow-twitch	11.96	118
Homozygous	Tubulin	Slow-twitch	7.97	79
Set #1				
Wild-type	Actin	Slow-twitch	5.16	100
Heterozygous	Actin	Slow-twitch	3.35	65
Homozygous	Actin	Slow-twitch	1.78	35
Wild-type	Actin	Slow-twitch	1.94	100
Heterozygous	Actin	Slow-twitch	1.89	97
Homozygous	Actin	Slow-twitch	1.10	56
Set #2				
Wild-type	Actin	Slow-twitch	2.06	100
Heterozygous	Actin	Slow-twitch	1.85	90
Homozygous	Actin	Slow-twitch	2.04	99

Wild-type	Actin	Slow-twitch	7.90	100
Heterozygous	Actin	Slow-twitch	19.60	248
Homozygous	Actin	Slow-twitch	4.45	56
Set #1				
Homozygous	Desmin	Fast-twitch	5.03	39
Wild-type	Desmin	Fast-twitch	12.77	100
Heterozygous	Desmin	Fast-twitch	7.42	58
Wild-type	Desmin	Fast-twitch	4.14	100
Heterozygous	Desmin	Fast-twitch	5.93	143
Homozygous	Desmin	Fast-twitch	5.23	126
Set #2				
Wild-type	Desmin	Fast-twitch	6.07	100
Heterozygous	Desmin	Fast-twitch	2.15	35
Homozygous	Desmin	Fast-twitch	2.27	37
Wild-type	Desmin	Fast-twitch	2.58	100
Heterozygous	Desmin	Fast-twitch	1.69	66
Homozygous	Desmin	Fast-twitch	2.12	82
Set #1				
Wild-type	Tubulin	Fast-twitch	13.79	100
Heterozygous	Tubulin	Fast-twitch	11.13	81
Homozygous	Tubulin	Fast-twitch	5.32	38
Wild-type	Tubulin	Fast-twitch	8.43	100
Heterozygous	Tubulin	Fast-twitch	5.68	67
Homozygous	Tubulin	Fast-twitch	8.24	98
Set #2				
Wild-type	Tubulin	Fast-twitch	3.01	100
Heterozygous	Tubulin	Fast-twitch	3.00	100
Homozygous	Tubulin	Fast-twitch	3.11	103
Wild-type	Tubulin	Fast-twitch	3.01	100
Heterozygous	Tubulin	Fast-twitch	3.77	125
Homozygous	Tubulin	Fast-twitch	1.59	53
Set #1				
Wild-type	Actin	Fast-twitch	4.20	100
Heterozygous	Actin	Fast-twitch	6.48	154
Homozygous	Actin	Fast-twitch	1.88	45
Wild-type	Actin	Fast-twitch	4.81	100
Heterozygous	Actin	Fast-twitch	3.24	67
Homozygous	Actin	Fast-twitch	2.94	61
Set #2				
Wild-type	Actin	Fast-twitch	2.30	100
Heterozygous	Actin	Fast-twitch	3.02	132
Homozygous	Actin	Fast-twitch	2.32	101
Wild-type	Actin	Fast-twitch	4.17	100
Heterozygous	Actin	Fast-twitch	3.23	77
Homozygous	Actin	Fast-twitch	1.46	35

Fluorescence Experiments.

	Type	DESMIN Observed Frequecy	TUBULIN Observed Frequency	ACTIN Observed Frequency
Genotype	**Wild-type**			
Fiber	Slow			
Pattern	No	0	10	12
Pattern	Yes	19	9	26
Fiber	Fast			
Pattern	No	15	46	67
Pattern	Yes	83	63	136
Genotype	**Heterozygous**			
Fiber	Slow			
Pattern	No	2	8	12
Pattern	Yes	8	15	19
Fiber	Fast			
Pattern	No	48	36	71
Pattern	Yes	104	68	185
Genotype	**Homozygous**			
Fiber	Slow			
Pattern	No	6	17	37
Pattern	Yes	9	17	12
Fiber	Fast			
Pattern	No	91	33	135
Pattern	Yes	31	30	50